Acoustics of Aircraft Engine-Duct Systems

ALI H. NAYFEH,* JOHN E. KAISER,† AND DEMETRI P. TELIONIS‡
Virginia Polytechnic Institute and State University, Blacksburg, Va.

I. Introduction

IN a broad classification, one may consider aircraft noise to be generated by either an internal or an external source. The externally generated noise is due primarily to the jet exhaust and the airframe itself. The internally generated noise is due primarily to the rotating turbomachinery blades[1-5] and to the combustion process.[6,7] To achieve lower specific fuel consumption, future aircraft engines are expected to have bypass ratios in the range of 4–6.[1] This results in a reduction of the jet noise to relatively insignificant proportions, but results in an increase of the fan noise. The over-all noise level of such engines without acoustic treatment is greater than the noise level of low bypass engines and consists of a broad band spectrum and high-pitched discrete frequency components.

The internal flowfield past the blades is generally unsteady due to the presence of upstream blades and vanes and turbulence. The interaction of this unsteady flow and the moving blades produces upstream and downstream traveling pressure waves (acoustic modes). Some of these modes decay naturally, while the others need to be suppressed by acoustically treating the engine ducts. To achieve noise reductions in the ducts without an economic penalty, the acoustic treatment must be optimized.

To achieve this optimization the complete engine is usually represented as a system of interacting elements, and then the elements of the duct are optimized for the lowest noise level. The effect of a sound-absorbing material is to attenuate some of the modes and to reflect others. Thus, these effects are accounted for by the large matrix equation[8]

$$\begin{bmatrix} \mathbf{T}_a & \mathbf{R}_b \\ \mathbf{R}_a & \mathbf{T}_b \end{bmatrix} \begin{bmatrix} \mathbf{A} \\ \mathbf{B} \end{bmatrix} = \begin{bmatrix} \text{sources} \end{bmatrix} \tag{1}$$

where the vectors $\mathbf{A}$ and $\mathbf{B}$ represent the downstream and upstream propagating modes, the matrices $\mathbf{T}$ and $\mathbf{R}$ represent the transmission and reflection factors and the subscripts a and b refer to the upstream and downstream modes. The purpose of the present paper is to critically survey the state-of-the-art regarding the methods of determining the transmission and reflection coefficients and the dependence of these coefficients on the material properties, duct geometry, and flowfield.

II. Acoustic Equations

Velocities, lengths, and time are made dimensionless using the ambient speed of sound c_a, a characteristic duct dimension d_o (such as the half width or radius for uniform ducts), and d_o/c_a, respectively. The pressure p is made dimensionless using $\rho_a c_a^2$, the density ρ and temperature T are made dimensionless using their corresponding ambient values, while viscosity μ and thermal conductivity κ are made dimensionless using their corresponding wall values. In terms of these dimensionless variables, the equations which describe the unsteady viscous flow in a duct are[9]:

conservation of mass

$$\partial\rho/\partial t + \nabla\cdot(\rho\mathbf{v}) = 0 \tag{2}$$

conservation of momentum

$$\rho\left(\frac{\partial\mathbf{v}}{\partial t} + \mathbf{v}\cdot\nabla\mathbf{v}\right) = -\nabla p + \frac{1}{R_e}\cdot\tau \tag{3}$$

conservation of energy

$$\rho\left(\frac{\partial T}{\partial t} + \mathbf{v}\cdot\nabla T\right) - (\gamma-1)\left(\frac{\partial p}{\partial t} + \mathbf{v}\cdot\nabla p\right) = \frac{1}{R_e}\left[\frac{1}{Pr}\nabla\cdot(\kappa\nabla T) + (\gamma-1)\Phi\right] \tag{4}$$

equation of state

$$p = \gamma\rho T \tag{5}$$

Ali Hasan Nayfeh is a Professor of Engineering Science and Mechanics at Virginia Polytechnic Institute and State University, Blacksburg, Virginia. His academic background includes a B.S. (1962) with Great Distinction in Engineering Science from Stanford University, and an M.S. (1963) and a Ph.D. (1964) in Aeronautics and Astronautics from Stanford University. He has conducted studies and published extensively in perturbation methods, aeroacoustics, lifting surface theory, hydrodynamic stability, surface waves, structural dynamics, nonlinear vibrations, electromagnetic waves, flight mechanics, and re-entry physics. He is the author of *Perturbation Methods*, Wiley-Interscience, 1973. He is a consultant to Sandia Laboratories and a member of Tau Beta Pi, Phi Beta Kappa, Sigma Xi, AIAA, and the American Physical Society.

John E. Kaiser is an Assistant Professor of Engineering Science and Mechanics at Virginia Polytechnic Institute and State University, Blacksburg, Virginia. He received his Ph.D. in Engineering Mechanics from Stanford University in 1968. His research interests include aeroacoustics and numerical computation of fluid flows, and he has a number of publications on duct acoustics. Dr. Kaiser is a member of the AIAA, Tau Beta Pi, Phi Kappa Phi, and Sigma Xi, and is an associate member of the Acoustical Society of America.

Demetri P. Telionis is an Associate Professor of Engineering Science and Mechanics at Virginia Polytechnic Institute, Blacksburg, Virginia. He received his undergraduate education at the National Technical University of Athens, Greece; the M.S. degree (1969) in Theoretical and Applied Mechanics and the Ph.D. degree (1970) in Aerospace Engineering, both from Cornell University. He has worked and published in time-dependent laminar and turbulent flows, separated flows, unsteady boundary-layer separation, and aeroacoustics. He is a member of the AIAA, Sigma Xi, and Democritos Society.

Presented as Paper 73-1153 at the joint CASI/AIAA Aeronautical Meeting, Montreal, Canada, October 29–30, 1973; submitted November 26, 1973; revised September 3, 1974. Work supported by NASA Langley Research Center under Grant NGR 47-004-109 and monitored by W. E. Zorumski.

Index category: Aircraft Noise, Powerplant.

* Professor, Engineering Science and Mechanics Department. Member AIAA.
† Assistant Professor, Engineering Science and Mechanics Department. Member AIAA.
‡ Associate Professor, Engineering Science and Mechanics Department. Member AIAA.

where γ is the gas specific heat ratio, τ is the dimensionless stress tensor, Φ is the dimensionless dissipation function, $Pr = \mu_w c_p/\kappa_w$ is the Prandtl number, and $R_e = \rho_a c_a d_o/\mu_w$ is the Reynolds number.

We assume that each flow quantity $q(\mathbf{r}, t)$ is the sum of a steady mean flow quantity $q_o(\mathbf{r})$ and an unsteady acoustic flow quantity $q_1(\mathbf{r}, t)$. Substituting these assumed expressions into Eqs. (2–5), eliminating the mean flow quantities, and neglecting nonlinear acoustic quantities, we obtain the following general acoustic equations

$$\frac{\partial \rho_1}{\partial t} + \nabla \cdot (\rho_o \mathbf{v}_1 + \rho_1 \mathbf{v}_o) = 0 \tag{6}$$

$$\rho_o\left(\frac{\partial \mathbf{v}_1}{\partial t} + \mathbf{v}_o \cdot \nabla \mathbf{v}_1 + \mathbf{v}_1 \cdot \nabla \mathbf{v}_o\right) + \rho_1 \mathbf{v}_o \cdot \nabla \mathbf{v}_o = -\nabla p_1 + \frac{1}{R_e} \nabla \cdot \boldsymbol{\tau}_1 \tag{7}$$

$$\rho_o\left(\frac{\partial T_1}{\partial t} + \mathbf{v}_o \cdot \nabla T_1 + \mathbf{v}_1 \cdot \nabla T_o\right) + \rho_1 \mathbf{v}_o \cdot \nabla T_o - (\gamma - 1)\left(\frac{\partial p_1}{\partial t} + \mathbf{v}_o \cdot \nabla p_1 + \mathbf{v}_1 \cdot \nabla p_o\right) = \frac{1}{R_e}\left[\frac{1}{Pr} \nabla \cdot (\kappa_o \nabla T_1 + \kappa_1 \nabla T_o) + (\gamma - 1)\Phi_1\right] \tag{8}$$

$$p_1/p_o = \rho_1/\rho_o + T_1/T_o \tag{9}$$

where $\boldsymbol{\tau}_1$ and Φ_1 are linear in the acoustic quantities.

Equations (6–9) are not valid for the study of high intensity sound (nonlinear wave propagation), which is discussed in Sec. VII; however, they are the basis of all studies discussed in the other sections of this paper. No solution to these equations subject to general initial and boundary conditions has been found for general mean flows. To determine solutions for the acoustic propagation in ducts, researchers have restricted their attention to two specific flow configurations: parallel mean flows and near-parallel mean flows. These are discussed below.

A. Parallel Mean Flows

In this flow configuration, the mean velocity is parallel to the duct axis and is a function of the coordinate normal to the duct walls. For two dimensional ducts having uniform cross section,

$$\mathbf{v}_o = u_o(y)\mathbf{e}_x, \quad \rho_o = \rho_o(y), \quad T_o = T_o(y)$$
$$\mu_o = \mu_o(y), \quad \kappa_o = \kappa_o(y), \quad \text{and} \quad p_o = \text{const}$$

where the x-axis coincides with the duct axis and the y-axis is normal to it (see Fig. 1). This flow configuration is often referred to as "fully-developed flow" by acousticians. In this case, Eqs. (6–9) become

$$\frac{\partial \rho_1}{\partial t} + u_o \frac{\partial \rho_1}{\partial x} + \rho_o\left(\frac{\partial u_1}{\partial x} + \frac{\partial v_1}{\partial y}\right) + \rho_o' v_1 = 0 \tag{10}$$

$$\rho_o\left(\frac{\partial u_1}{\partial t} + u_o \frac{\partial u_1}{\partial x} + u_o' v_1\right) = -\frac{\partial p_1}{\partial x} + \frac{1}{R_e}\left\{\mu_o\left(\frac{\partial^2 u_1}{\partial x^2} + \frac{\partial^2 u_1}{\partial y^2}\right) + \frac{1}{3}\mu_o \frac{\partial}{\partial x}\left(\frac{\partial u_1}{\partial x} + \frac{\partial v_1}{\partial y}\right) + \mu_o'\left(\frac{\partial u_1}{\partial y} + \frac{\partial v_1}{\partial x}\right) + \mu_1 u_o'' + u_o' \frac{\partial \mu_1}{\partial y}\right\} \tag{11}$$

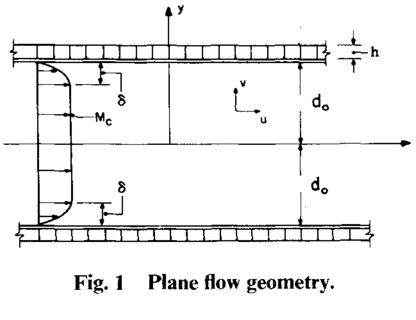

Fig. 1 Plane flow geometry.

$$\rho_o\left(\frac{\partial v_1}{\partial t} + u_o \frac{\partial v_1}{\partial x}\right) = -\frac{\partial p_1}{\partial y} + \frac{1}{R_e}\left\{\mu_o\left(\frac{\partial^2 v_1}{\partial x^2} + \frac{\partial^2 v_1}{\partial y^2}\right) + \frac{1}{3}\mu_o \frac{\partial}{\partial y}\left(\frac{\partial u_1}{\partial x} + \frac{\partial v_1}{\partial y}\right) + \mu_o' \frac{\partial u_1}{\partial x} + \frac{2}{3}\mu_o'\left(2\frac{\partial v_1}{\partial y} - \frac{\partial u_1}{\partial x}\right)\right\} \tag{12}$$

$$\rho_o\left(\frac{\partial T_1}{\partial t} + u_o \frac{\partial T_1}{\partial x} + T_o' v_1\right) - (\gamma - 1)\left(\frac{\partial p_1}{\partial t} + u_o \frac{\partial p_1}{\partial x}\right) = \frac{1}{R_e}\left\{\frac{1}{Pr}\left[\kappa_o \frac{\partial^2 T_1}{\partial x^2} + \frac{\partial}{\partial y}\left(\kappa_o \frac{\partial T_1}{\partial y} + \kappa_1 T_o'\right)\right] + (\gamma - 1)\left[2u_o'\mu_o\left(\frac{\partial u_1}{\partial y} + \frac{\partial v_1}{\partial x}\right) + \mu_1 u_o'^2\right]\right\} \tag{13}$$

$$p_1/p_o = \rho_1/\rho_o + T_1/T_o \tag{14}$$

Three approaches have been used to solve Eqs. (10–14) subject to boundary and initial conditions. In one approach,[10,11] Fourier and Laplace transforms are employed to solve simplified forms of these equations. In the second approach,[12,13] a Green's function is used to study the cases of uniform and no mean flows. In the third approach, the solution is sought in the form

$$p_1 = \sum_{n=-\infty}^{\infty} A_n \psi_n(y) e^{i(k_n x - \omega t)} \tag{15}$$

where $\psi_n(y)\exp[i(k_n x - \omega t)]$ are the normal-mode solutions of Eqs. (10–14) subject to the given boundary conditions, k_n is the complex wave number, and ω is the dimensionless frequency. Once these modes are known, A_n can be obtained from the initial conditions at $x = x_o$. This approach assumes that the normal modes are a complete set. Using Fourier transforms to study inviscid acoustic propagation for the case in which u_o is analytic and does not vanish at the boundary, Möhring[11] suggested that algebraically growing modes of the form $\psi_n(y) f(x) \exp(i\omega t)$ might exist. Using asymptotic expansions, Nayfeh and Telionis[14] showed that algebraically growing modes do not exist when $R_e \to \infty$ if critical layers (locations at which $ku_o = \omega$) do not exist. This result is an indirect proof that the normal modes are a complete set provided that all eigenvalues, k_n, are distinct. Moreover, Shankar[10] found that his solution, obtained by Fourier and Laplace transforms, agreed with the normal-mode approach. Tester[13] and Zorumski and Mason[15] have shown that multiple roots of the eigenvalue equation do exist under certain conditions. If $k_m = k_s$, the contributions to Eq. (15) by the m and s modes take the form[15]

$$(A_m + A_s x)\psi_m(y)\exp[i(k_m x - \omega t)]$$

The normal-mode description is the most frequently used method in the literature and is adopted in the remainder of this paper.

Since the problem formulated in this section is linear, one can determine the normal modes independently of each other. To this end we let

$$u_1 = u(y)E, \quad v_1 = v(y)E, \quad p_1 = p(y)E,$$
$$T_1 = T(y)E, \quad \rho_1 = \rho(y)E, \quad \mu_1 = \mu(y)E,$$
$$\kappa_1 = \kappa(y)E,$$

where

$$E = \exp[i(kx - \omega t)]$$

Substituting these expressions into Eqs. (10–14), we obtain

$$i(ku_o - \omega)\rho + ik\rho_o u + \frac{d}{dy}(\rho_o v) = 0 \tag{16}$$

$$i(ku_o - \omega)u + u_o' v + \frac{ik}{\rho_o} p = \frac{1}{\rho_o R_e}\left\{\frac{d}{dy}\left[\mu_o\left(\frac{du}{dy} + ikv\right)\right] + \frac{2}{3}ik\mu_o\left(2iku - \frac{dv}{dy}\right) + \frac{d}{dy}(u_o'\mu)\right\} \tag{17}$$

$$i(ku_o - \omega)v + \frac{1}{\rho_o}\frac{dp}{dy} = \frac{1}{\rho_o R_e}\left\{\frac{d}{dy}\left[\frac{2}{3}\mu_o\left(2\frac{dv}{dy} - iku\right)\right] + ik\mu_o\left(\frac{du}{dy} + ikv\right) + iku_o'\mu\right\} \tag{18}$$

$$i(ku_o-\omega)T+T_o'v-\frac{i(\gamma-1)}{\rho_o}(ku_o-\omega)p=$$
$$\frac{1}{\rho_o R_e}\left\{\frac{1}{Pr}\left[-k^2\kappa_o T+\frac{d}{dy}\left(\kappa_o\frac{dT}{dy}+\kappa T_o'\right)\right]+\right.$$
$$\left.(\gamma-1)\left[2u_o'\mu_o\left(\frac{du}{dy}+ikv\right)+\mu u_o'^2\right]\right\} \quad (19)$$

$$p/p_o=\rho/\rho_o+T/T_o \quad (20)$$

No solution to Eqs. (16–20), which include the effects of viscosity and heat conduction on the acoustic wave, has yet been obtained. Except for studies of the acoustic boundary layer (see Sec. IV) researchers have assumed an inviscid acoustic disturbance. Neglecting the viscous terms (i.e., letting $R_e\to\infty$), we can combine Eqs. (16–20) into the following equation for p:

$$\frac{d^2p}{dy^2}-\left(\frac{2ku_o'}{u_o k-\omega}-\frac{T_o'}{T_o}\right)\frac{dp}{dy}+\left[\frac{(u_o k-\omega)^2}{T_o}-k^2\right]p=0 \quad (21)$$

Equation (21) includes the effects of both velocity and temperature gradients in the mean flow.

If the temperature of the mean flow is assumed to be constant, u_o becomes the local Mach number M, and Eq. (21) reduces to the equation obtained by Pridmore-Brown[16]:

$$d^2p/dy^2+[2kM'/(\omega-Mk)](dp/dy)+[(Mk-\omega)^2-k^2]p=0 \quad (22)$$

For uniform mean flows, Eq. (22) reduces further to

$$d^2p/dy^2+[(Mk-\omega)^2-k^2]p=0 \quad (23)$$

In cylindrical geometry, the normal modes have the form

$$q_1=q(r)\exp[i(kx-\omega t+m\theta)] \quad (24)$$

where (r,θ,x) is the cylindrical coordinate system with the x-axis coinciding with the duct axis (see Fig. 2), q stands for any of the flow quantities, and m is an integer. In this case, the equations corresponding to Eqs. (21–23) are

$$\frac{d^2p}{dr^2}+\left(\frac{1}{r}+\frac{T_o'}{T_o}-\frac{2ku_o'}{ku_o-\omega}\right)\frac{dp}{dr}+\left[\frac{(ku_o-\omega)^2}{T_o}-k^2-\frac{m^2}{r^2}\right]p=0 \quad (25)$$

$$\frac{d^2p}{dr^2}+\left(\frac{1}{r}+\frac{2kM'}{\omega-Mk}\right)\frac{dp}{dr}+\left[\left(Mk-\omega\right)^2-k^2-\frac{m^2}{r^2}\right]p=0 \quad (26)$$

$$\frac{d^2p}{dr^2}+\frac{1}{r}\frac{dp}{dr}+\left[(Mk-\omega)^2-k^2-\frac{m^2}{r^2}\right]p=0 \quad (27)$$

Effects of parallel mean flows are discussed in Sec. IV while effects of temperature gradients are discussed in Sec. V.

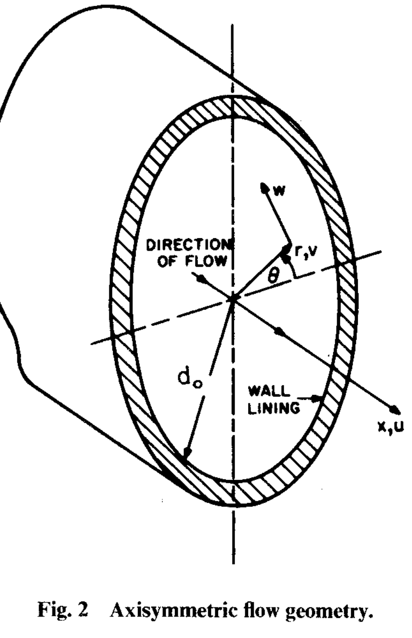

Fig. 2 Axisymmetric flow geometry.

B. Near-Parallel Mean Flows

In this case, the mean flow is assumed to deviate by a small amount from a parallel flow. To express this deviation, we let

$$\mathbf{v}_o=u_o(x_1,y)\mathbf{e}_x+\varepsilon v_o(x_1,y)\mathbf{e}_y,\quad \rho_o=\rho_o(x_1,y),\quad T_o=T_o(x_1,y),\quad p_o=p_o(x_1) \quad (28)$$

where ε is a small parameter characterizing the nonparallelism of the mean flow so that $x_1=\varepsilon x$ is a slow axial scale. We assume that normal modes of the form of Eq. (15) still exist but with slowly varying amplitudes A_n and wave numbers k_n. Thus, we use the method of multiple scales,[17] and assume normal modes of the form

$$p_1=p(y,x_1;\,\varepsilon)E,\quad v_1=v(y,x_1;\,\varepsilon)E$$
$$u_1=u(y,x_1;\,\varepsilon)E,\quad \rho_1=\rho(y,x_1;\,\varepsilon)E \quad (29)$$
$$T_1=T(y,x_1;\,\varepsilon)E$$

where $E=\exp(i\phi)$ such that

$$\partial\phi/\partial t=-\omega \quad \text{and} \quad \partial\phi/\partial x=k(x_1) \quad (30)$$

Substituting Eqs. (28–30) into Eqs. (6–9) and letting $R_e\to\infty$, we obtain

$$i(ku_o-\omega)\rho+ik\rho_o u+\frac{\partial}{\partial y}(\rho_o v)=-\varepsilon\left[\frac{\partial}{\partial x_1}(\rho_o u+u_o\rho)+\rho\frac{\partial v_o}{\partial y}\right] \quad (31)$$

$$i(ku_o-\omega)u+v\frac{\partial u_o}{\partial y}+\frac{ik}{\rho_o}p=-\varepsilon\left[\frac{\partial}{\partial x_1}(u_o u)+v_o\frac{\partial u}{\partial y}+\frac{\rho}{\rho_o}\times\left(u_o\frac{\partial u_o}{\partial x_1}+v_o\frac{\partial u_o}{\partial y}\right)\right] \quad (32)$$

$$i(ku_o-\omega)v+\frac{1}{\rho_o}\frac{\partial p}{\partial y}=-\varepsilon\left[u_o\frac{\partial v}{\partial x_1}+\frac{\partial}{\partial y}(v_o v)\right]-\varepsilon^2\left[u\frac{\partial v_o}{\partial x_1}+\frac{\rho}{\rho_o}\left(u_o\frac{\partial v_o}{\partial x_1}+v_o\frac{\partial v_o}{\partial y}\right)\right] \quad (33)$$

$$iku_o-\omega)T+\frac{\partial T_o}{\partial y}v-i\frac{(\gamma-1)}{\rho_o}(ku_o-\omega)p=$$
$$-\varepsilon\left[u_o\frac{\partial T}{\partial x_1}+v_o\frac{\partial T}{\partial y}+u\frac{\partial T_o}{\partial x_1}-(\gamma-1)\times\left(u_o\frac{\partial p}{\partial x_1}+v_o\frac{\partial p}{\partial y}+u\frac{\partial p_o}{\partial x_1}\right)\right] \quad (34)$$

$$p/p_o=\rho/\rho_o+T/T_o \quad (35)$$

Letting $\varepsilon\to 0$, we find that Eqs. (31–35) reduce to the inviscid parts of Eqs. (16–20). Solutions of these equations are discussed in Sec. VI.

III. Duct-Liner Acoustic Properties

Lining materials have been used as sound absorbers in architectural designs and industrial installations for some time. However, the extreme temperature and pressure environment in the interior of a jet engine has recently required extensive experimental and theoretical research to develop appropriate liners. The desirable mechanical properties of such liners are diverse and rather stringent. Liners should have minimum thickness and weight, should be able to resist high pressure levels, face extreme temperature differences, and of course should have sufficient ability to absorb sound. These liners are usually a combination of perforated sheets, cavities and pieces of porous materials.[18,19] In the sections that follow we describe briefly some of the commonly used liners as well as the theoretical models developed to explain and predict the effectiveness of their operation.

A. Liner Designs and Their Properties

In a broad classification, liners can be divided into point-reacting (locally-reacting) and bulk-reacting liners. Point-reacting liners are by definition liners that permit propagation

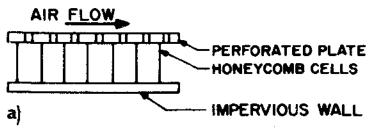

Fig. 3a Perforated-plate, honeycomb liner.

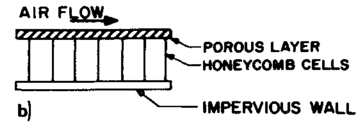

Fig. 3b Resistive resonator liner.

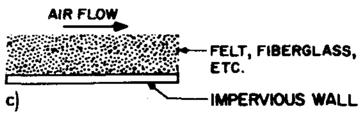

Fig. 3c Bulk-reacting liner.

only in the direction normal to the duct wall. Such liners are the most common in practice because they are easy to manufacture and possess desirable structural properties. They usually consist of a perforated sheet or a thin layer of porous material followed by a honeycomb core and backed by the impervious wall of the duct (see Figs. 3a, b). The honeycomb core is made up of narrow cavities of usually polygonal shape that are directed perpendicular to the wall and the facing sheet and act as resonators.[20] Honeycomb cells are usually manufactured with metal ribbons, bonded or welded at nodes, to form a variety of cell sizes and shapes. The perforated-plate and honeycomb liners (Fig. 3a) are sharply tuned resonators effective over a narrow frequency range when used in low airflow velocities or low SPL (sound pressure levels). However, they provide a broader band-width attenuation at high SPL. The porous-sheet-honeycomb liners (resistive-resonator) can yield substantial attenuations over a wide frequency range by a proper choice of the material and geometry parameters.

Bulk-reacting liners are liners that permit propagation in more than one direction. Such liners may consist of isotropic or anisotropic porous materials. These liners may not have the ability to attenuate high levels of discrete sound but they attenuate broad-band noise and low frequency noise more effectively. However, the available materials are not suitable for use in an aircraft engine owing to their poor mechanical properties and their tendency to absorb fluids.

The broad-band resistive-resonator linings are the most widely used. Porous materials are constructed by sintering fiber-metal sheets or woven-screen metal sheets or continuous-filament metal sheets.[21] Some porous materials are constructed by weaving fiber-glass into sheets of variable thickness.

There is a series of mechanical and acoustical tests routinely performed[22–24] but due to space limitations these tests are not described here.

B. Flow Through Porous Materials

Fluid flow through porous materials has been extensively studied since the middle of the previous century (see Irmay[25] for Refs.). For steady flow the well known Darcy's law states

$$\nabla p + \sigma \mathbf{v} = 0 \tag{36}$$

where σ is a constant that we call resistivity. This form of the momentum equation has been extended to unsteady flows and therefore acoustic disturbances by several authors. Unfortunately, there is very little agreement on the notation and very often on the form of the coefficients of the governing equations. The continuity and momentum equations in their most acceptable form read[26–30]

$$\Omega \frac{\partial \rho}{\partial t} + \rho_o \nabla \cdot \mathbf{v} = 0 \tag{37}$$

$$\rho_e \frac{\partial \mathbf{v}}{\partial t} + \sigma \mathbf{v} + \nabla p = 0 \tag{38}$$

where $\mathbf{v}$ is the average acoustic velocity through the porous medium, Ω is the porosity, σ is the resistivity and ρ_e is the effective density. Throughout Secs. III-B and III-C, equations and variables are in dimensional form, unless specifically stated otherwise.

The porosity Ω is usually defined as the ratio of the void volume to the total bulk volume of the porous material. The resistivity σ is the same quantity that appears in the steady form of the equation. The governing equations in Refs. 26–30 can be brought more or less into the same form. However, the equation used by Tack and Lambert,[31] even after it is expressed in terms of the average velocity, shows some discrepancies if compared with Eqs. (37–38).

The quantity σ is found in various publications represented by different symbols and referred to by various terms. Scott[26] uses the symbol r and the term "resistance coefficient," Morse and Ingard[27] use the symbol Φ and the term "flow resistance," Zwikker and Kosten[28] use the symbol σ and the term "resistance constant," Tack and Lambert[31] use the symbol r and the term "resistivity," and Bies[32] uses the symbol R and the term "flow resistivity." In general, σ is not a constant but a function of the velocity. Green and Duwez[33] assume that

$$\sigma = \alpha\mu + \beta\rho|\mathbf{v}| \tag{39}$$

where α and β are independent of the fluid properties and are functions of the mechanical properties of the porous material such as the specific permeability, porosity, frontal surface ratio, and structure factor. The linear part of the resistivity is due to viscous resistance, whereas the nonlinear part is due to inertia effects. At low velocities, σ corresponds to Darcy's constant, while at high velocities it corresponds to Forchheimer's formula.[25]

The effective density is usually expressed as

$$\rho_e = s\rho_o/\Omega \tag{40}$$

where s is a structure factor which accounts for the apparent increase in the air density owing to the structural properties of the material and the constrictions and blind passages.[28]

At least three independent constants are needed in order to describe the unsteady flow of a particular fluid through a porous medium. It is more convenient and more accurate to measure directly the resistivity and effective density instead of calculating them via viscosity, porosity, and various material constants.[32,34]

To complete the fluid flow description, the acoustic pressure and density are usually related by the equation of state

$$p_1 = \rho_1 c_e^2 \tag{41}$$

where c_e is generally a complex quantity[27,32] and is referred to as the effective speed of sound. It is real only in the limiting cases of high and low frequencies. At low frequencies, up to about 100 Hz, the temperature of the porous material remains essentially the same during a cycle owing to the large thermal capacity of the material; consequently, the compression and rarefaction take place slowly enough for the gas to be isothermal and

$$c_e^2 = \mathscr{R}T \tag{42}$$

where $\mathscr{R}$ is the ideal gas constant. On the other hand, at high frequencies, down to about 1000 Hz, the compression and rarefaction take place so rapidly that there is no heat exchange between the gas and the material. Consequently, the motion is adiabatic and

$$c_e^2 = \gamma \mathscr{R} T \tag{43}$$

where γ is the gas specific heat ratio.

In Eq. (38), the porous material is assumed to be homogeneous and isotropic. Whereas the homogeneous assumption may be reasonable, the isotropic assumption is not valid, in general, because the resistivity and structure factor of a fibrous material normal to the plane of the fibers are larger than those in their plane.[35,36] Consequently, ρ_e and σ are, in general, second-order

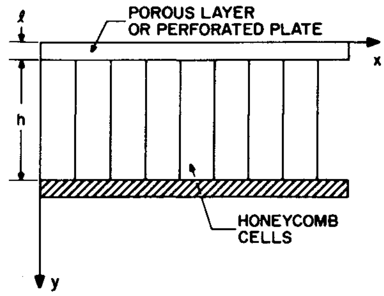

Fig. 4 Coordinate system for a point reacting liner.

tensors rather than scalars. For example, in two-dimensional flows, Eq. (38) can be written in Cartesian coordinates as

$$\begin{bmatrix} \rho_{e11} & \rho_{e12} \\ \rho_{e21} & \rho_{e22} \end{bmatrix} \begin{bmatrix} \frac{\partial u}{\partial t} \\ \frac{\partial v}{\partial t} \end{bmatrix} + \begin{bmatrix} \frac{\partial p}{\partial x} \\ \frac{\partial p}{\partial y} \end{bmatrix} + \begin{bmatrix} \sigma_{11} & \sigma_{12} \\ \sigma_{21} & \sigma_{22} \end{bmatrix} \begin{bmatrix} u \\ v \end{bmatrix} = 0 \tag{44}$$

C. Impedances of Liners

1) Liners with linear acoustic properties

To determine the impedance of a point-reacting liner with linear acoustic properties, we introduce a Cartesian coordinate system (see Fig. 4) and proceed as follows. The impedance of the liner consists of contributions from both the cavity and the porous facing sheet. The impedance of the cavity at the cavity/sheet interface is[27]

$$i\rho_w c_w \cot(\omega h/c_w)$$

where the subscript w refers to the wall. The manner in which the contribution from the porous facing sheet has been modeled in the literature depends on the thickness of the porous material, as discussed below.

a) Liners with thin materials: The impedance of a liner composed of a thin porous material or perforated plate backed by a cavity is

$$Z = \Delta Z + i\rho_w c_w \cot(\omega h/c_w) \tag{45}$$

where ΔZ is the impedance change across the porous sheet or perforated plate. For a time harmonic variation of the form $\exp(-i\omega t)$, $\partial v/\partial t = -i\omega v$ and Eq. (38) becomes

$$\partial p/\partial y + (\sigma - i\omega\rho_e)v = 0 \tag{46}$$

Integrating Eq. (46) from $y = 0$ to $y = l$, we obtain

$$p(l) - p(0) + \int_o^l (\sigma - i\omega\rho_e)v\, dy = 0 \tag{47}$$

Since l is very small, v is approximately constant across the porous material or the plate and Eq. (47) becomes

$$p(l) - p(0) + (\sigma - i\omega\rho_e)lv = 0$$

Hence,

$$\Delta Z = (\sigma - i\omega\rho_e)l$$

The specific acoustic impedance z is defined by

$$z = Z/\rho_w c_w \tag{48}$$

and can be expressed in terms of dimensionless quantities as

$$z = R[(1 - (i\omega/\omega_o)] + i\cot(\omega h/c_w) \tag{49}$$

where $R = \sigma l/\rho_w c_w$ is the flow resistance and $\omega_o = \sigma d_o/\rho_e c_a$ is the characteristic frequency of the facing sheet. In practice, R and ω_o are determined experimentally. Within the literature, the impedance of the facing sheet/cavity liner is usually described by Eq. (49). However, for liners with thick facing sheets, it is necessary to consider a more general equation.[37] In addition, perforated plates generally behave in a nonlinear manner.

Liners consisting of more than one layer of the thin-facing-sheet, backing-cavity combination have been examined experimentally by Atvars and Mangiarotty[24] and theoretically by Zorumski,[38] Mariano,[39] and Ko.[40]

b) Liners with thick materials: If l is not small compared with h, we determine ΔZ by solving the equations of motion in the porous material. Thus, we let

$$p = f(y)\exp(-i\omega t), \qquad v = g(y)\exp(-i\omega t)$$

in Eqs. (37) and (38), eliminate ρ using Eq. (41), and obtain

$$g' - (i\Omega\omega/\rho_w c_e^2)f = 0 \qquad f' + (\sigma - i\rho_e\omega)g = 0 \tag{50}$$

The solution of Eq. (50) is

$$f = a\cos(k_y y + \phi_o)$$

$$g = [ak_y/(\sigma - i\rho_e\omega)]\sin(k_y y + \phi_o) \tag{51}$$

where a and ϕ_o are constants and

$$k_y^2 = i\Omega\omega(\sigma - i\rho_e\omega)/\rho_w c_e^2 \tag{52}$$

Hence, the impedance in the porous material is

$$Z_m = [(\sigma - i\rho_e\omega)/k_y]\cot(k_y y + \phi_o) \tag{53}$$

The phase ϕ_o is obtained by equating Z_m to the impedance of the cavity at $y = l$. The result is

$$\phi_o = -k_y l + \arctan\left[\frac{(\sigma - i\rho_e\omega)}{i\rho_w c_w k_y}\tan\frac{\omega h}{c_w}\right] \tag{54}$$

Consequently, the specific impedance of the liner is[37]

$$z = [(\sigma - i\rho_e\omega)/\rho_w c_w k_y]\cot\phi_o \tag{55}$$

Kaiser, Shaker, and Nayfeh[37] showed that, except for very thin facing sheets, a large error may be introduced if one uses Eq. (49).

c) Bulk liners: For the two-dimensional bulk-reacting liner, shown in Fig. 3c, an analysis similar to the previous leads to the specific impedance of Eqs. (54) and (55) provided that k_y is given by[36,41]

$$k_y^2 = -k^2 + i\Omega\omega(\sigma - i\rho_e\omega)/\rho_w c_e^2 \tag{56}$$

Scott[26] analyzed the effect of isotropic bulk-reacting liners on the wave propagation in two-dimensional ducts in the absence of mean flow. His theory was verified by a number of investigators in Refs. 34, 35, and 42–44. Kurze and Vér[36] extended the analysis of Scott by considering anisotropic bulk-reacting liners. Their results show that, for low frequencies, the optimum attenuation of the lowest mode is achieved by a bulk-reacting liner whose resistivity in the axial direction increases with frequency, in agreement with the experimental observations of Bokor.[35,42] Nayfeh, Sun, and Telionis[41] analyzed the effect of isotropic bulk-reacting liners on the wave propagation in two-dimensional and circular ducts carrying sheared mean flow. Their results show that considerable error may be introduced by treating a bulk-reacting liner as a point-reacting liner.

2) Liners with nonlinear acoustic properties

Measured data in typical aircraft engines indicate that the noise intensity is the order of 160 db, and the acoustic properties of the liners are no longer independent of the SPL at these intensities. The appropriate nonlinear impedance of a thin porous sheet or perforated plate is still unresolved (see, for example, Ref. 45 for a review and new results). Rice[46] has examined the nonlinear resistance of Helmholtz resonators by analyzing the interaction of jets from the resonator orifices with the mean flow. A semi-empirical formula has been proposed by Zorumski and Parrott[47] relating the pressure drop across the sheet or plate and the acoustic velocity as

$$\Delta p = \left[R(v_1) + \chi(v_1)\frac{\partial}{\partial t}\right]v_1 \tag{57}$$

where $R(v_1)$ is independent of the sound frequency while χ is a function of the test frequency.

D. Boundary Conditions

1) Hard wall

At a hard wall, the appropriate boundary conditions are

$$\mathbf{v}_1 \cdot \mathbf{n} = 0 \tag{58a}$$

$$\mathbf{v}_1 - (\mathbf{v}_1 \cdot \mathbf{n})\mathbf{n} = 0 \tag{58b}$$

$$T_1 = 0 \tag{58c}$$

where **n** is a unit vector normal to the wall and the wall is assumed to be kept at a constant temperature. Equation (58a) expresses the fact that the fluid cannot penetrate the wall while Eq. (58b) represents the no-slip condition. For an inviscid acoustic disturbance, Eq. (58b) cannot be satisfied, in general, and the inviscid acoustic solution is not valid in a thin layer called the "acoustic boundary layer" (see Sec. IV-C).

2) *Lined wall*

The boundary conditions (58b) and (58c) are applicable to point-reacting liners. For bulk-reacting liners, the condition (58b) is replaced by an expression of continuity of the shear stress. However, the boundary condition (58a) needs to be replaced by a new condition for both types of liners. For a no-slip mean flow, all investigators agree that the appropriate condition is the continuity of the normal velocity; that is,

$$\mathbf{v}_1 \cdot \mathbf{n} = \mathbf{v}_p \cdot \mathbf{n} \tag{59}$$

where the subscript p refers to the liner. On the other hand, considerable discussion has appeared in the literature as to whether continuity of particle displacement or continuity of normal velocity is the appropriate boundary condition to use when the mean velocity is taken to be nonzero at the wall. In discussing the transmission and reflection of plane waves at an interface between two moving fluids, Miles[48] and Ribner[49] derived a boundary condition based on the continuity of particle displacement and pointed out that earlier studies using continuity of normal velocity were incorrect. Ingard[50] used the particle displacement formulation in his discussion of reflection at a solid boundary, and Gottlieb[51] set up a simple computational test in a linear shear layer to demonstrate that the particle displacement was the appropriate boundary condition at a mean-flow discontinuity. Nevertheless, reports that experimental results were adequately predicted by the attenuation from a uniform profile with continuity of normal velocity[52] maintained the question as a topic of interest. Tack and Lambert[31] compared predictions with experimental results and concluded that neither form of the boundary condition when used with a uniform profile was adequate over a range of flow conditions but that they were "... inclined to believe that (continuity of particle displacement) is a more correct boundary condition for the uniform flow solution ...." However, their results show that continuity of normal velocity is reasonably accurate over a certain frequency range, and they conclude that it should be more useful in that frequency range than continuity of particle displacement. Mungur and Plumblee[53] compared theoretical results from a uniform profile using the two boundary conditions with the theoretical results of a shear profile of several thicknesses. As the thickness became smaller, the shear-profile results exhibited a trend toward the particle-displacement results. A more detailed examination of the numerical limit as the boundary-layer thickness vanishes was presented by Savkar.[54] Unfortunately the results approached a value slightly different from the particle displacement result—probably a consequence of the limitations of the method of solution that was used (see Sec IV on the Ritz-Galerkin procedure). Recently, Eversman and Beckemeyer[55] and Tester[56] used the method of matched asymptotic expansions to show that the shear-profile results approach, in the limit of vanishing boundary-layer thickness, the results of a uniform profile with continuity of particle displacement at the wall. Nayfeh, Kaiser and Shaker[57] confirmed numerically the conclusion of Refs. 55 and 56. Hence, the appropriate boundary condition is

$$\xi = \xi_p \tag{60}$$

where ξ is the particle displacement.

The boundary condition (60) can be interpreted as follows. Because the uniform-mean-flow model assumes that the viscous layers are vanishingly thin, the viscous layers should be modeled as vortex sheets that separate the regions of uniform flow within the duct and within the porous liners. These vortex sheets comply with the waves propagating in the duct-liner configuration. Thus, if $F(\mathbf{r}, t) = 0$ is the equation describing the location of a vortex sheet, the boundary condition (60) is equivalent to

$$\frac{\partial F}{\partial t} + \mathbf{v} \cdot \nabla F = 0 \quad \text{at} \quad F = 0 \tag{61a}$$

$$\frac{\partial F}{\partial t} + \mathbf{v}_p \cdot \nabla F = 0 \quad \text{at} \quad F = 0 \tag{61b}$$

which states that any particle on the vortex sheet remains on it for all times. For the special case, $F(\mathbf{r}, t) = y - \xi(x, t) = 0$, Eqs. (61) become

$$v = \partial\xi/\partial t + u\,\partial\xi/\partial x \quad \text{at} \quad y = \xi \tag{62a}$$

$$v_p = \partial\xi/\partial t + u_p(\partial\xi/\partial x) \quad \text{at} \quad y = \xi \tag{62b}$$

Linearizing Eqs. (62), we have

$$v_1 = \partial\xi/\partial t + u_o\,\partial\xi/\partial x \quad \text{at} \quad y = 0 \tag{63a}$$

$$v_{1p} = \partial\xi/\partial t + u_{op}\,\partial\xi/\partial x \quad \text{at} \quad y = 0 \tag{63b}$$

It should be emphasized that the conclusion that the continuity of particle displacement is the appropriate boundary condition is based on the assumption that the acoustic boundary-layer thickness vanishes faster than the mean boundary-layer thickness (all the theoretical studies cited above[48-57] assumed an inviscid acoustic disturbance). If these thicknesses are the same order, the appropriate boundary condition is still an open question.

In addition to the above conditions, the acoustic pressure must be continuous across the vortex sheet; that is,

$$p_1 = p_{1p} \tag{64}$$

For a harmonic wave,

$$\xi = \xi_o \exp[i(kx - \omega t)]$$

where ξ_o is a constant and Eqs. (63) become

$$v = i(ku_o - \omega)\xi_o, \qquad v_p = i(ku_{op} - \omega)\xi_o \tag{65}$$

Eliminating ξ_o from Eqs. (65) and using Eq. (64), we have

$$\frac{p}{v} = \frac{(ku_{op} - \omega)p_p}{(ku_o - \omega)v_p} \tag{66}$$

Using the expression for the impedance in Eq. (48), we rewrite Eq. (66) as

$$\frac{p}{v} = \frac{ku_{op} - \omega}{ku_o - \omega}\rho_w c_w z \tag{67}$$

Using the inviscid part of Eq. (18), we express Eq. (67) as

$$\frac{dp}{dy} + \frac{i(ku_o - \omega)^2}{c_w(ku_{op} - \omega)}\beta p = 0 \tag{68}$$

where the specific acoustic admittance $\beta = 1/z$.

For a point-reacting liner or a bulk-reacting liner with no mean flow, Eq. (68) becomes

$$\frac{dp}{dy} - \frac{i(ku_o - \omega)^2}{c_w \omega}\beta p = 0 \tag{69}$$

For a uniform mean temperature, $c_w = 1$ and Eq. (69) becomes

$$dp/dy - [i(kM - \omega)^2/\omega]\beta p = 0 \tag{70}$$

For a no-slip mean flow, Eq. (69) becomes

$$dp/dy - (i\omega/c_w)\beta p = 0 \tag{71}$$

which, for a uniform mean temperature, reduces to

$$dp/dy - i\omega\beta p = 0 \tag{72}$$

Equations (69–72) are applicable at the upper wall of a plane duct and at the outer wall of an annular duct. At the lower or inner walls, the signs of the β terms must be changed.

IV. Effect of Parallel Flow and Viscosity

The influence of the mean flow on sound propagation in a duct has been the subject of a large number of investigations that are discussed below. Two counteracting effects have been identified and examined in these investigations. The first is convection, which refers to the tendency of the mean flow to carry the acoustic wave with it at its local speed, and the second is refraction, which refers to the tendency of transverse

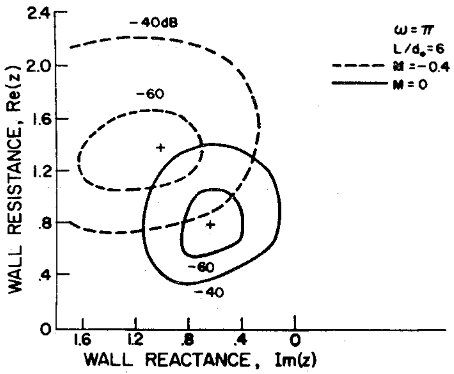

Fig. 5 Effect of Mach number on attenuation; from Ref. 58.

gradients in the mean flow to induce a wave motion normal to the duct centerline.[10,31] The relative magnitudes of these two influences depend upon the mean velocity and temperature profiles. If a uniform mean flow is assumed, only the convective effect will be present, and the governing equations are simpler to solve than in the more general case. A discussion of the results of studies which examine solely the convective influence is given in Sec. IV-A. The results of studies which include the effects of refraction and the methods of solution employed in these studies are examined in Sec. IV-B.

A. Uniform-Flow Case

Several investigations[50,58-61] have been concerned with examining the convective effects produced by a uniform mean flow. Such an approximation to the mean flow should be a reasonable model for cases of very thin boundary layers, provided the particle-displacement boundary condition is used.

For a plane duct, the problem to be solved is given by Eq. (23) subject to a boundary condition of the form of Eq. (70) at $y = 1$ and a boundary condition at the duct centerline:

$$p'(0) = 0, \qquad \text{symmetric modes,} \tag{73a}$$

or

$$p(0) = 0, \qquad \text{antisymmetric modes} \tag{73b}$$

The solution to Eqs. (23) and (73) is given by

$$p(y) = \begin{cases} A_n \cos k_y y, & \text{symmetric modes} \\ A_n \sin k_y y, & \text{antisymmetric modes} \end{cases} \tag{74}$$

where

$$k_y{}^2 = (Mk - \omega)^2 - k^2 \tag{75}$$

Substitution of Eq. (74) into Eq. (70) yields

$$k_y \tan k_y + (i\beta/\omega)(Mk - \omega)^2 = 0 \tag{76a}$$

for symmetric modes and

$$k_y \cot k_y - (i\beta/\omega)(Mk - \omega)^2 = 0 \tag{76b}$$

for antisymmetric modes. Thus, for uniform mean flow, the problem reduces to the solution of a pair of algebraic equations, either (76a) and (75) or (76b) and (75). Noting the periodic nature of both (76a) and (76b), we can set

$$k_y = \frac{n\pi}{2} + \lambda, \qquad n = \begin{cases} 0, 2, 4, \ldots \text{symmetric modes} \\ 1, 3, 5, \ldots \text{antisymmetric modes} \end{cases} \tag{77}$$

and reduce Eqs. (76) to a single equation

$$\left(\frac{n\pi}{2} + \lambda\right) \tan \lambda + \frac{i\beta}{\omega}(Mk - \omega)^2 = 0 \tag{78}$$

where

$$k = \{-\omega M + [\omega^2 - (1 - M^2)(n\pi/2 + \lambda)^2]^{1/2}\}/(1 - M^2) \tag{79}$$

To examine all cases of upstream and downstream propagation, we can consider $M > 0$ and use both the positive and negative roots of the radical in Eq. (79), or we can use only the positive root and take the Mach number to be positive for downstream propagation and negative for upstream propagation. The two approaches are equivalent, and the latter is used here. For hard walls, $\beta \to 0$, and the solution of Eq. (78) is simply $\lambda = 0$ or $k_y = n\pi/2$, $n = 0, 1, 2, \ldots$. Thus,

$$k = \{\omega M + [\omega^2 - (1 - M^2)(n\pi/2)^2]^{1/2}\}/(1 - M^2)$$

The nondimensional hard-wall cutoff frequency is then given by

$$\omega = (1 - M^2)^{1/2} n\pi/2$$

For frequencies above this value, the attenuation rate, $Im(k)$, is zero, and for frequencies below this value attenuation occurs without the use of liners. Conversely, only those modes for which

$$n\pi/2 < \omega/(1 - M^2)^{1/2}$$

are of interest, since the higher modes are naturally cut off. In lined ducts a similar cutoff frequency occurs, but its precise value is difficult to calculate numerically.

The formulation of the problem in the manner outlined above is due to Ingard[50] who examined propagation between two parallel plane boundaries, one rigid and one with finite specific impedance and derived the basic eigenvalue equations (75) and (76a) for symmetric modes. A numerical analysis of these equations was not performed, but he did obtain an asymptotic expression for the attenuation of the fundamental mode ($n = 0$) by perturbing the equations about the hard-wall case:

$$Im(k) = \frac{Re(\beta)}{2} \frac{1}{(1 + M)^2}$$

where $|\beta| \ll 1$. Hence, to the first approximation, only the resistive characteristic of the liner contributes to the attenuation. This result also shows that the upstream-propagating wave ($M < 0$) is attenuated more than the downstream-propagating wave ($M > 0$).

For propagation in annular ducts, Eq. (27) is solved subject to a boundary condition of the form of Eq. (70) at each wall. The solution of Eq. (27) is given by

$$p(r) = A_n[J_m(k_r r) + B_n Y_m(k_r r)] \tag{80}$$

where

$$k_r{}^2 = (Mk - \omega)^2 - k^2 \tag{81}$$

and J_m and Y_m are the Bessel functions of order m of the first and second kinds, respectively.

For the case of a circular duct, we must take $B_n = 0$ to obtain finite pressures at $r = 0$. In this case, the boundary condition at the outer wall yields

$$k_r J'_m(k_r) = (i\beta/\omega)(Mk - \omega)^2 J_m(k_r)$$

or

$$k_r J_{m+1}(k_r) = [m - (i\beta/\omega)(\omega - kM)^2] J_m(k_r) \tag{82}$$

which, together with (81), defines the problem for the eigenvalues k_r and the complex wave number k. Axially symmetric modes are obtained from $m = 0$, and more complex circumferential modes are obtained from higher values of m. For each circumferential mode, there are an infinite number of solutions to Eq. (82); the problem is similar to that posed by the plane

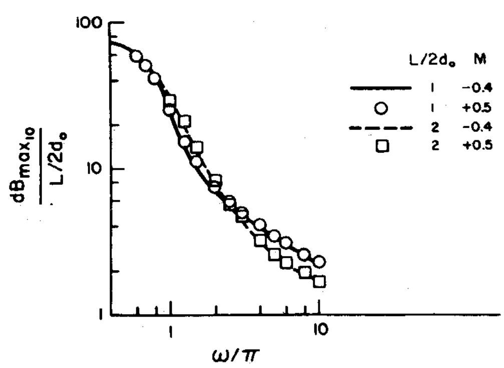

Fig. 6 Maximum attenuation as a function of frequency; from Ref. 58.

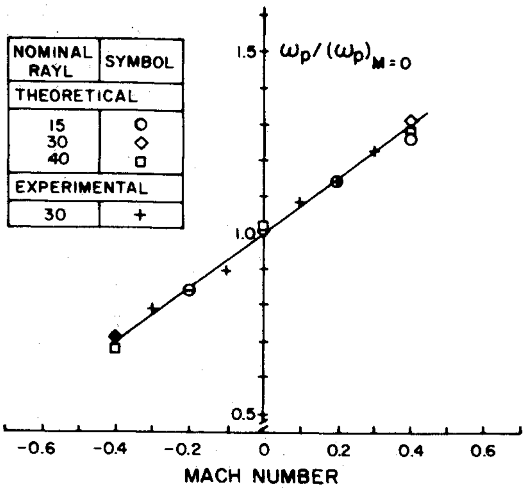

Fig. 7 Comparison of theoretical and experimental results for peak-attenuation frequency; $h = 0.0834$, $\omega_o = 2000\pi/c_a$; from Ref. 60.

case except that the repetitive nature of the solutions is not as easily expressed as it is in Eq. (78).

For a hard wall and no mean flow in an annular duct of inner radius r_1, Eqs. (80) and (81) give the wavenumber k as

$$k = (\omega^2 - k_r^2)^{1/2}$$

where k_r is the cutoff frequency and is the solution to $J_m'(k_r)Y_m'(k_r r_1) = J_m'(k_r r_1)Y_m'(k_r)$. If $\omega < k_r$, the waves are attenuated without the use of a liner. This observation was first noted by Tyler and Sofrin,[62] who related the shaft frequency Ω_s and the number of blades B to the sound frequency $\omega = B\Omega_s$ and the circumferential mode number $m = B$ to obtain

$$k = B[M_m^2 - (k_r/B)^2]^{1/2}$$

where M_m is Mach number of the blade tips. Thus, the rotating pressure pattern due to a single rotor will propagate only if the blade-tip Mach number exceeds a critical value. The critical value was shown to be greater than unity and approached unity as $r_1 \to 1$ and/or $m \to \infty$. Tyler and Sofrin also demonstrated that the pressure pattern produced by a rotor-stator interaction would contain supersonic, propagating components even when the rotor tip speed is subsonic. Hence, current engine designs minimize the interaction noise by omission of inlet guide vanes and use of single-stage fans and large spacing between the rotor and the exit guide vanes.[63]

Inclusion of the uniform axial mean flow in Eq. (81) leads to cutoff (see, for example, Ref. 64) if

$$M^2 + \omega^2/k_r^2 < 1$$

or, for a single rotor, if

$$M_m < k_r(1 - M^2)^{1/2}/B$$

Rice[58] examined the propagation of an initially plane pressure wave in a cylindrical duct. The initial wave was approximated by a combination of the first 10 axially symmetric modes, and the sound power attenuation was calculated over a finite length L. Special attention was given to the optimization of the liner properties. For example, in Fig. 5 contours of constant sound attenuation are shown in the liner specific impedance plane for two values of the mean Mach number and a fixed frequency. The liner properties required for maximum attenuation clearly depend upon the mean Mach number. However, Rice found that the maximum attenuation level that can be achieved is practically independent of the Mach number, as shown in Fig. 6, but does depend strongly on the wave frequency—the higher the frequency the smaller the attenuation levels that can be achieved. Rice discussed both the particle-displacement and the normal-velocity boundary conditions at the wall and apparently used the latter. Whether this affects the general conclusion based on Fig. 6 is not clear without conducting the complete set of numerical computations again.

Doak and Vaidya[59] considered propagation in lined circular ducts with mean flow (also considered were annular, circular, rectangular, and arbitrary cross sections with no mean flow). A detailed discussion of the identification of the eigenvalues, i.e., the roots of Eq. (82), for all modes was included. Their approach used a perturbation about either the hard-wall case, $J_m'(k_r) = 0$, or the "pressure-release" case, $J_m(k_r) = 0$. Although their uniform-mean-flow results are invalidated by their use of continuity of normal velocity at the wall, the main thrust of the paper, which is the location of all roots of the eigenvalue equation, is quite instructive.

Eversman[60] and Ko[61] have examined propagation in lined rectangular ducts with two rigid walls and two lined walls, and set up the eigenvalue equation for the general (m, n) mode. However, the results of numerical computations were presented for only the plane modes ($m = 0$), i.e., solutions of Eqs. (78) and (79) were presented. Both investigations considered a liner consisting of a porous facing sheet backed by cellular air cavities for which the impedance is described by Eq. (49). The air cavity gives a narrow-band peak attenuation which nominally occurs at quarter-wave-length resonance, and the resistance of the facing sheet provides a broader band attenuation about the peak attenuation (or tuning) frequency. However, both investigations show that the tuning frequency for a specified liner depends upon the Mach number, just as Rice found that the liner properties for peak attenuation at given frequency depended upon the Mach number.

Eversman[60] limited his analysis to the fundamental mode ($n = 0$) for the purpose of determining the variation of the tuning frequency with Mach number. Figure 7 shows a comparison of the predicted peak-attenuation frequency ω_p with experimental data for a polymide liner whose resistance is 30 rayls. The results are in excellent agreement, and the theoretical results are rather insensitive to the resistance value that is chosen. Thus, the tuning frequency appears to be a function only of the cavity depth and the mean-flow Mach number. Experimental data presented by Eversman for other types of facing sheets show considerably more scatter, but the 30-rayl theoretical results still fit the experimental trend quite well.

Ko[61] examined the first 25 plane modes ($m = 0$; $n = 0, 1, \ldots, 25$) in the rectangular duct. Figure 8 shows the distinct identification

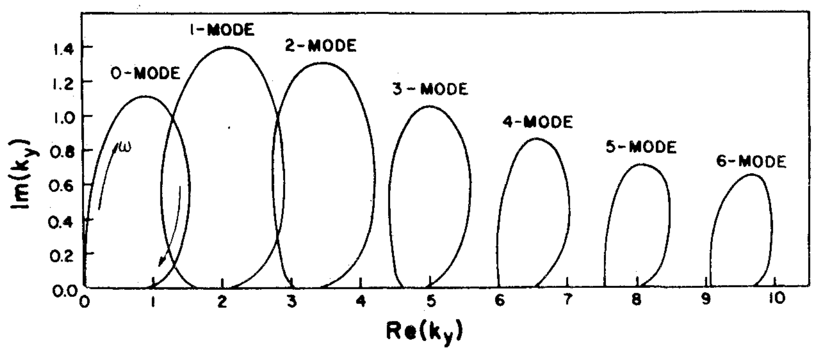

Fig. 8 Eigenvalues of first seven modes; $M = 0.36$, $R = 2$, $\omega_o = 56.3$, $h = 0.06748$; from Ref. 61.

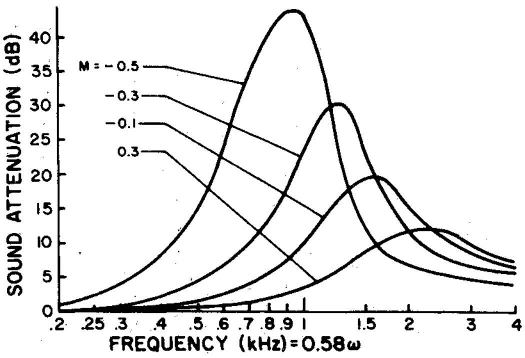

Fig. 9 Effect of mean Mach number on the sound attenuation; $R = 1.5$, $\omega_o = 25.9$, $h = 0.271$, $L/d_o = 4.34$; from Ref. 61.

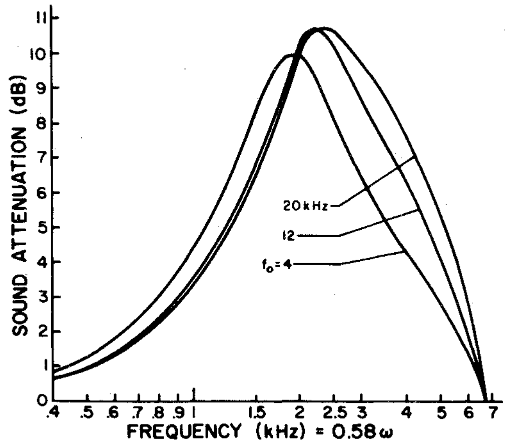

Fig. 11 Effect of characteristic frequency of acoustic lining material on the sound attenuation; $M = 0.4$, $R = 1.5$, $f_o = 0.58\omega_o$, $h = 0.271$, $L/d_o = 4.34$; from Ref. 61.

of modes that occurs when Eqs. (78) and (79) are solved for k_y by varying the frequency with n fixed. For upstream propagation these eigenvalue loops, though distinct and well defined, are not as orderly as those shown by Ko. The sound power attenuation of each of the modes was determined and then combined into a total sound attenuation, assuming approximately equal amplitudes for the modal energy distribution [$A_n^2/Re(k_y)\,Im(k_y)$ equal to a const for all modes]. An extensive and thorough parametric survey was conducted of the effects of Mach number, duct height, and liner properties, and a comparison of theoretical and experimental results for a Boeing 747/JT9D engine under a variety of operating conditions was given. Figure 9 shows the effect of Mach number on the attenuation over a range of frequencies. The peak in the attenuation curve is a consequence of the duct liner properties, as previously discussed. Both the convective effect on the attenuation level (decreasing attenuation for downstream propagation and increasing for upstream propagation) and the shift in the tuning frequency are clearly shown. Thus, a knowledge of the mean-flow operating conditions is essential to the design of optimum linears. Figure 10 demonstrates the effect of the liner resistance on the bandwidth about the tuning frequency. The effect of the characteristic frequency of the liner, ω_o, is less pronounced but increasing values of ω_o broadens the bandwidth somewhat, as shown in Fig. 11. In Fig. 12, the essential role of the cavity depth in controlling the tuning frequency is demonstrated.

Ko's comparison of theoretical and experimental data produced generally good agreement for the exhaust duct (downstream propagation) and an over-prediction of attenuation for the inlet duct, a result that was attributed to the omission of the refractive effects of the mean boundary layer.

B. Nonuniform, Parallel Mean Flows

The presence of gradients in the mean velocity profile produces a refraction of the sound wave whose importance has been demonstrated in numerous studies that are discussed below. The equations that are solved in such studies are Eq. (22) for plane ducts and Eq. (26) in circular ducts, subject to the boundary conditions discussed in Sec. IV-A.

For the developing boundary-layer flows that occur in engine-duct systems, the transverse mean velocity component is nonzero, an effect that has been neglected in the equations cited above. Thus, the application of Eqs. (22) or (26) to the flow in engine-duct systems constitutes a "quasi-parallel" approximation. The attenuation is calculated at each streamwise station using the local boundary-layer profile but neglecting the effect of the growing boundary layer. The techniques of studying nonparallel mean flows is examined in Sec. VI.

Since the coefficients in the differential equations are variable, no closed-form solutions are available, and approximations using either numerical or perturbation techniques are required. A description of the methods of solution is contained in Sec. IV-B, 1) and followed in Sec. IV-B, 2) by a discussion of the results of the investigations of the effects of a shear profile on acoustic propagation in a duct.

1) *Methods of solution*

Although the methods of solution that are discussed here were developed for a study of the effects of velocity gradients,

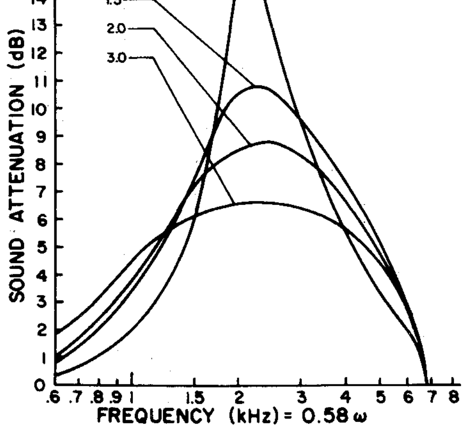

Fig. 10 Effect of acoustic resistance on the sound attenuation; $M = 0.4$, $\omega_o = 25.9$, $h = 0.271$, $L/d_o = 4.34$; from Ref. 61.

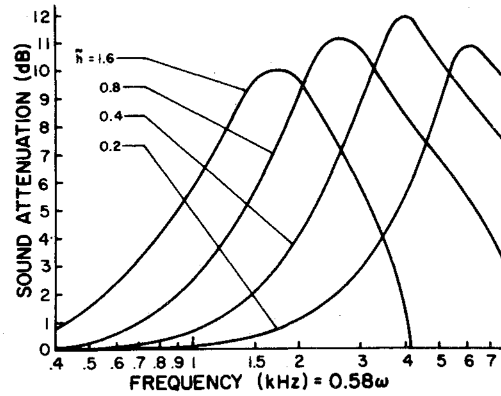

Fig. 12 Effect of acoustic lining depth on the sound attenuation; $M = 0.4$, $R = 1.5$, $\omega_o = 25.9$, $L/d_o = 4.34$, $h = 0.271\bar{h}$; from Ref. 61.

i.e., a study of Eqs. (22) or (26), they are usually applicable to cases of nonuniform temperature as well. Thus, in this section, the methods of solution are frequently discussed in the context of application to Eqs. (21) and (25).

a) Asymptotic expansions: Several authors have applied techniques of perturbation analysis to the solution of the eigenvalue problem for acoustic propagation. The first such analysis was given by Pridmore-Brown,[16] who derived the governing equation for the acoustic pressure in a rectangular duct in the form of Eq. (22) and analysed the cases of a linear mean-velocity profile and a $\frac{1}{7}$th power-law profile. Using the "turning-point" analysis of Langer (p. 339, Ref. 17), he obtained asymptotic solutions, which are valid for large values of the frequency, in terms of the Airy integrals.[65] With these solutions, Pridmore-Brown demonstrated that the refractive effects of the mean velocity gradient were large and that these effects were greater at higher frequencies; his results showed a sound pressure level at the wall as large as 90 db greater than at the center of the duct for $\omega = 20$ and a centerline Mach number, M_c, equal to 0.5.

Pridmore-Brown's solution for the $\frac{1}{7}$th power-law profile is not valid at the wall, a fact that led to criticism of his analysis. However, it should be noted that the basic difficulty lies not with the method of analysis but with the choice of the $\frac{1}{7}$th power law to describe the mean flow. The use of this formula leads to an infinite shear at the wall that is totally unrealistic and introduces a singularity that is difficult to handle by any analysis. Analytically, the singularity is integrable, as shown by Eversman.[66] However, with numerical methods, considerable care is required to obtain accurate solutions, and even when the singularity is removed by use of a linear sublayer at the wall, the numerical effort required for a forward-integration solution (section 1b) is considerable.[57]

Tack and Lambert,[31] who were interested in examining the frequency spectrum $\omega < 1/\delta$, where δ is the dimensionless boundary-layer thickness, proposed a different analytic approach, in which the Mach number is used as the independent variable and the solution is obtained as a power series in M. The radius of convergence of such a solution extends to the singularity at $Mk-\omega = 0$, i.e. to the "critical layer." The authors encountered some difficulty with inaccuracy for the upstream propagation cases and attributed this to the fact that the critical layer occurs closer to $M = 0$ for upstream propagation than it does for downstream propagation. In general, the authors expressed disappointment with the solution thus obtained because the calculated effect of refraction was not as large as those measured in their experiments.

Eversman and Beckemeyer[55] and Tester[56] have obtained solutions within the mean boundary-layer region by expanding the acoustic pressure in an asymptotic series for small values of the boundary-layer thickness δ. Following Eversman and Beckmeyer, we let

$$\eta = 1 - r/\delta$$

and

$$M(r) = M_c\phi(\eta), \qquad \phi(0) = 0, \qquad \phi(1) = 1$$

and expand the acoustic pressure into

$$p(\eta) = p_o(\eta) + \delta p_1(\eta) + \delta^2 p_2(\eta) + \dots$$

Calculation of $p(\eta)$ to $0(\delta^2)$ and evaluation of $(dp/dr)/p$ at $y = 1-\delta$ yields

$$(dp/dr)/p = \frac{\left(1 - M_c\frac{k}{\omega}\right)^2 \left\{ i\beta\omega + \delta\left[\alpha_1 - \alpha_2 \int_o^1 \frac{d\xi}{[1 - M_c\phi(k/\omega)]^2}\right]\right\}}{1 - \delta i\beta\omega \int_o^1 \left(1 - M_c\phi\frac{k}{\omega}\right) d\xi} \quad \text{at} \quad y = 1-\delta \qquad (83)$$

where

$$\alpha_1 = i\beta\omega + \omega^2, \qquad \alpha_2 = k^2 + m^2$$

In the limit as $\delta \to 0$, Eq. (83) reduces to a statement of the continuity of particle displacement at the wall, verifying the appropriate boundary condition for the case of uniform mean flow. Equation (83) can also be used as the outer boundary condition for the known analytic solution, Eq. (80), within the uniform core, and in numerical tests for small values of δ, it has yielded accurate answers.[55,67] An analysis of this type was used by Eversman[66] to obtain solutions for the $1/N$ power-law mean profile. Beckemeyer[68] has extended the previous analysis to include the effect of transverse temperature and density gradients in the mean flow.

Other asymptotic approximations have been suggested by Hersh and Catton[69] and by Shankar.[10] For hard-wall ducts, Hersh and Catton expand the eigenvalue k and the eigenfunction $p(y)$ in asymptotic series in powers of M_c, the centerline Mach number. This expansion about the plane-wave mode propagating in a medium at rest was solved to $0(M_c^2)$, and the results were compared with their more accurate computations made with a forward-integration technique. Reasonable agreement for small values of M_c and ω worsened as M_c increased (for obvious reasons) and as ω increased since the basic expansion process assumed that $\omega = 0(1)$.

Shankar[10] also considered propagation in hard-walled ducts and assumed that the mean flow was given by

$$M(y) = M_o + \varepsilon M_1(y), \qquad \varepsilon \ll 1$$

and therefore used ε as the perturbation parameter. The solution was developed for arbitrary values of M_o, but numerical calculations were obtained only for $M_o = 0$. Thus the basic perturbation technique is closely related to that used by Hersh and Catton; however, Shankar did not apply the technique to the normal-mode form of the equations, i.e., he did *not* assume, a priori, that the solution was of the variable-separable form, Eq. (15). Instead, he considered an initial-value problem in which a harmonic disturbance was generated at $x = 0$ in an initially quiescent medium, and in which Eqs. (10–14) with $Re \to \infty$ governed the acoustic disturbance. Asymptotic solutions for $\varepsilon \to 0$ were obtained using Fourier and Laplace transforms for both transient and large time conditions. The zeroth-order solution was a plane pressure disturbance travelling in a uniform mean flow. Thus, Shankar's solution, as well as that of Hersh and Catton, represents a perturbation about plane-wave propagation. To the order considered, it was found that the solution was composed of the superposition of wave modes, in which the variables did separate. Thus, the solution was consistent with the normal-mode approach.

In general, the limitations on the accuracy of the perturbation methods offset any advantage that they have over the more accurate numerical methods that are described below. An exception is the use of Eq. (83) for small values of the boundary-layer thickness to reduce the problem to an equivalent one with uniform mean flow. This could result in a substantial reduction in computational effort, provided that efficient and accurate routines are available for the computation of Bessel functions of complex arguments (see, for example, Ref. 70). In addition, the equivalent uniform-mean-flow approach simplifies the identification of modes—an area that frequently proves bothersome with numerical methods.

b) Forward-integration methods: Equations (21) and (25) can be rewritten as a pair of first-order ordinary differential equations of the form

$$dP_1/dY = P_2$$

and (84)

$$dP_2/dY = f(Y, P_1, P_2;\ k)$$

where P_1 represents the acoustic pressure p, P_2 represents the first derivative of p, and Y represents either y or r depending on whether a plane or circular duct is being considered. The function $f(Y, P_1, P_2;\ k)$ is

$$f(Y, P_1, P_2;\ k) = -\left[\frac{j}{Y} + \frac{T_o'}{T_o} + \frac{2ku_o'}{\omega - ku_o}\right]P_2 - \left[\frac{(\omega - ku_o)^2}{T_o} - k^2 - \frac{jm^2}{Y^2}\right]P_1$$

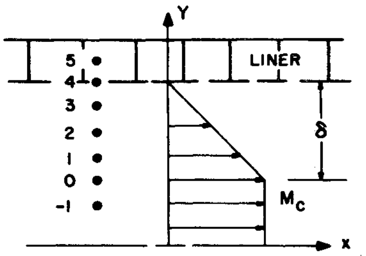

Fig. 13 Grid points in the central-difference method of Refs. 39, 40, 79 and 80.

where

$$j = \begin{cases} 0 & \text{plane ducts} \\ 1 & \text{axisymmetric ducts} \end{cases}$$

Equations (84) can be solved numerically as an initial-value problem if both P_1 and P_2 are known at some initial station. Since the amplitude of the eigenfunction is arbitrary, one initial value, either $P_1(0)$ or $P_2(0)$, can be selected arbitrarily. The second value is then obtained from application of Eqs. (73) in plane ducts, or Eq. (69) in an annular duct, or a condition obtained from $p(r) \to J_m(k,r)$ as $r \to 0$ in circular ducts. In the circular-duct case, the use of forward-integration techniques requires that the initial condition be transferred to a point located ΔY from the centerline in order to avoid the singularities in $f(Y, P_1, P_2; k)$. The asymptotic behavior of the Bessel function for small arguments provides the necessary information for this transfer (see, for example, Ref. 71).

With both initial values known and with the use of an assumed value for the eigenvalue, k, Eqs. (84) can be integrated with any of a large number of numerical schemes. At the outer wall, $Y = 1$, a check is made to determine whether Eq. (69) is satisfied. Then, a Newtonian iteration on the value of k is performed until this boundary condition is satisfied to some specified accuracy.

The mode to which the solution converges in such an analysis depends upon the initial guess that is used for k. This feature is probably the greatest problem that is encountered with numerical methods of solution. The usual approach is to use a known analytic solution for uniform mean flow or no mean flow to provide initial convergence to the desired mode at a given frequency.[71] Subsequent calculations then increment the value of the frequency, or the Mach number, or the boundary-layer thickness, and the eigenvalue k is required to be a continuous function of these parameters. Such calculations can become somewhat tedious; thus Mikhail and Abdelhamid[72] suggest the use of an effective Mach number together with the uniform-flow solution as a quick method to obtain $Re(k)$.

The use of a forward integration method was first suggested by Mungur and Gladwell[73] who used a fourth-order Runge-Kutta method. The simplicity of this method, its stability, and its accuracy—truncation errors are $0(\Delta Y^5)$—have lead to its adoption in several subsequent investigations (see Refs. 53, 57, 69, 71, 74, 75); a predictor-corrector method (which was not described) was used in Refs. 76 and 77.

c) Central-difference methods: For the discussion in this section it is convenient to write Eqs. (21) and (25) in the general form

$$\frac{d^2p}{dY^2} + f(Y;\, k)\frac{dp}{dY} + g(Y;\, k)p = 0 \tag{85}$$

where Y represents either y or r for plane or axisymmetric ducts, respectively. Hence

$$\begin{aligned} f(Y;\, k) &= \frac{2kM'}{\omega - kM} + \frac{T_o'}{T_o} + \frac{j}{Y} \\ g(Y;\, k) &= \frac{(\omega - kM)^2}{T_o} - k^2 - \frac{jm^2}{Y^2} \end{aligned} \tag{86}$$

where

$$j = \begin{cases} 0 & \text{plane ducts} \\ 1 & \text{axisymmetric ducts} \end{cases}$$

For application of central-difference procedures, the governing equation is evaluated at discrete grid points in the interval of interest, and the finite-difference quotients

$$\begin{aligned} \left.\frac{dp}{dY}\right|_n &= \frac{p_{n+1} - p_{n-1}}{2\Delta Y} \\ \left.\frac{d^2p}{dY^2}\right|_n &= \frac{p_{n+1} - 2p_n + p_{n-1}}{\Delta Y^2} \end{aligned} \tag{87}$$

are used to reduce the problem to the solution of a set of algebraic equations.

An elementary central-difference approach was used by Kurze and Allen[78] to examine the propagation of symmetric modes in a rectangular duct. Although the finite-difference quotients are second-order accurate, their analysis used large step sizes and thus the accuracy is suspect.

Mariano[39,79] and Ko[40,80] have employed a method in which the finite-difference procedure is applied only across the mean-boundary-layer region to provide a modified boundary condition for the known analytic solution, Eq. (74) or (80), in the uniform-flow region. The finite-difference configuration is shown in Fig. 13. Equation (85) is evaluated at the grid points $n = 1, 2, 3, 4$ and, with use of Eq. (87), yields four algebraic equations for six unknowns $p_o, p_1, \ldots, p_5$. A finite-difference form of the boundary condition at the wall provides a fifth algebraic equation. These equations are then solved to obtain p_1 in terms of p_o:

$$p_1 = s_o p_o \tag{88}$$

The algebraic details of obtaining s_o may be found in Refs. 79 or 80. At the edge of the boundary layer, the first derivative of p is represented by Eq. (87)

$$\left.\frac{dp}{dY}\right|_o = \frac{p_1 - p_{-1}}{2\Delta Y}$$

Rearranging terms and substituting Eq. (88) gives

$$s_o p_o = 2\Delta Y \left(\frac{dp}{dY}\right)_o + p_{-1} \tag{89}$$

All information from the mean shear profile is contained in the coefficient s_o, and the known solution in the uniform-flow region, Eq. (74) or (80), is used to evaluate p_o, $(dp/dY)_o$, and p_{-1} in terms of Bessel functions or sine and cosine functions. Equation (89) then provides the eigenequation which is solved for the eigenvalues k. The truncation errors of the finite-difference quotients of Eqs. (87) are $0(\Delta Y^2)$. Thus, the truncation errors of this method are $0(\delta^2)$, and for thin boundary layers the solutions should be accurate.

The relation of numerical solutions of this type to solutions based on the use of Eq. (83) has been discussed by Mariano.[81]

Kaiser[82] has proposed an approach that permits the use of an arbitrary number of grid points in the region of interest

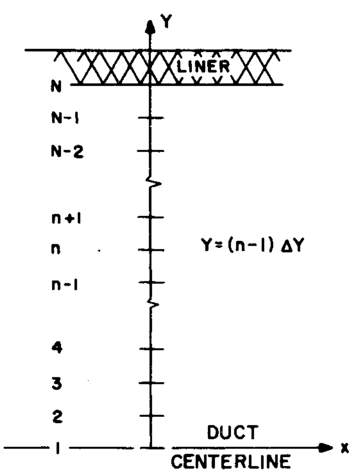

Fig. 14 Grid points in the central-difference scheme of Ref. 82.

(see Fig. 14). Equations (85) and (87) yield a set of algebraic equations of the form

$$A_n p_{n+1} + B_n p_n + C_n p_{n-1} = D_n, \qquad n = 2, 3, \ldots, N-1 \tag{90}$$

D_n is identically zero for the parallel-flow cases considered in this section but has been included in Ref. 82 to permit application to nonparallel flow situations.

The addition of a boundary condition at $Y = 0$ and the arbitrary specification of p_N completes the set, giving N equations for the unknowns $p_1, p_2, \ldots, p_N$. The coefficient matrix of these algebraic equations is tridiagonal, and thus the solution of the simultaneous equations is easily obtained by a standard algorithm, occasionally called the Thomas algorithm, for the inversion of tridiagonal matrices.[83] A Newtonian iteration on the value of k is performed until the calculated pressures satisfy the outer boundary condition [a finite-difference formulation of Eq. (69)] to a desired degree of accuracy. Truncation errors are $0(\Delta Y^2)$ or $0(1/N^2)$ throughout.

Kaiser applied both the central-difference scheme and the Runge-Kutta scheme to uniform flow in a plane duct so that comparisons with the exact solution could be used to assess the accuracy of each. For moderate accuracy requirements, [errors of $0(10^{-3})$], differences are slight, with Runge-Kutta being more efficient for the simpler lower modes and the central-difference procedure being more efficient for the more complex higher modes. For high-accuracy requirements [errors of $0(10^{-5})$], Runge-Kutta is clearly superior.

The central difference procedure may be the most desirable for a study of the fully viscous acoustic equations that can be obtained from Eqs. (16–20) with finite values of the Reynolds number—a study that has not yet been attempted. This sixth-order system of equations and the corresponding boundary conditions represent a two-point boundary-value problem. Thus, the use of a forward-integration process would require iteration on the initial conditions as well as on the value of the complex wave number. Although the additional iteration is easily accomplished as a consequence of the linearity of the equations, the central-difference procedure may well prove to be the simplest to apply.

d) Ritz-Galerkin procedure: For the discussion of this section it is convenient to represent the acoustic pressure equation in the form

$$L(p) = 0 \tag{91}$$

where L is the appropriate linear operator from any of the four Eqs. (21), (22), (25) or (26).

The application of the Ritz-Galerkin procedure requires that the acoustic pressure be approximated by a polynomial

$$p(y) \cong p_n(y) = \sum_{j=0}^{n} a_j \phi_j(y) \tag{92}$$

where $\phi_j(y)$ are a linearly independent set of basis functions that individually satisfy the boundary conditions. Various suggestions for the choice of these basis functions have been made by Hersh and Catton,[69] Savkar,[54] and Unruh and Eversman.[84,85]

The assumed pressure profile, Eq. (92) is substituted into Eq. (91), and the resulting equation is multiplied by ϕ_m and integrated across the duct to obtain

$$\int_o^1 L[p_n(y)]\phi_m(y)\,dy = 0$$

This equation then can be written in the form

$$\sum_{j=0}^{n} D_{mj} a_j = 0, \qquad m = 0, 1, 2, \ldots \tag{93}$$

where

$$D_{mj} = \int_o^1 \phi_m(y) L[\phi_j(y)]\,dy$$

Equations (93) provide a set of homogeneous algebraic equations for a_j which has a nontrivial solution only if the determinant $|D_{mj}|$ vanishes. Thus

$$|D_{mj}| = 0 \tag{94}$$

provides the constraint from which the value of the complex wave number k is determined.

The success of such an approach depends on the accuracy with which the actual acoustic pressure is represented by the selected polynomial expression. Hersh and Catton used $n = 12$ and reported that the eigenvalues were accurate to four decimal places. They then refined their answers with the Runge-Kutta method. Savkar used either $n = 1$ or $n = 2$ for his calculations; with no mean flow, the use of $n = 1$ yielded a complex wave number that differed from the exact value in the fourth significant figure; however, with a shear profile, the complex wave numbers obtained from $n = 1$ and $n = 2$ differed from one another in the second or third significant figure depending upon the Mach number.

Unruh and Eversman[84] thoroughly tested the convergence and accuracy of the Ritz-Galerkin method by comparing the results to those obtained from the Runge-Kutta procedure. They concluded that the method is a good alternative to the Runge-Kutta procedure, being superior for some applications but requiring caution in other instances. In particular, parametric studies at constant frequency of the effect of flow variables on the propagation of several modes can be accomplished very efficiently. However, at high frequency, Unruh and Eversman found, as did Hersh and Catton earlier, that the pressure profile of the fundamental mode was slow to converge even though an accurate value of the eigenvalue had been obtained. In addition, at low frequencies, computation of the higher modes requires a large number of basis functions.

Application of the Ritz-Galerkin procedure to rectangular ducts with boundary layers on all four walls was examined by Unruh and Eversman.[85]

2) *Effect of transverse velocity gradients*

The use of the methods of solution discussed above to solve Eqs. (22) and (26) requires that the variation of the Mach number across the duct be specified. Since the effort involved in calculating the actual mean-velocity profile is substantial, all investigations of the effect of shear layers on sound propagation have used various approximations for the mean flow, e.g., linear [see Refs. 10, 16, 39, 40, 54, 57, 69, 73, 74, 79, 80, 84, 85], quarter sine [see Refs. 53, 55, 66, 71, 76, 77], quadratic [see Refs.

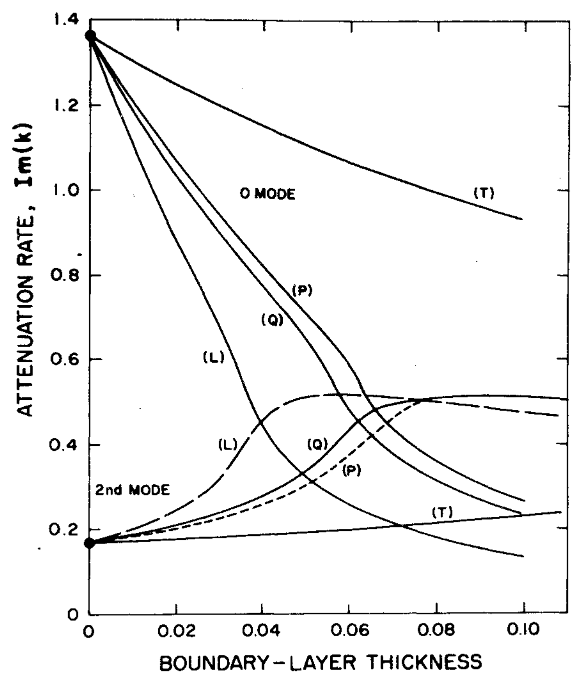

Fig. 15 Attenuation vs boundary-layer thickness for several profile shapes: (L) linear, (Q) quadratic, (P) Pohlhausen, (T) $\frac{1}{7}$th power-law; $M_c = -0.36$, $\omega = 5$, $R = 2$, $\omega_o = 56.3$, $h = 0.06748$; from Ref. 57.

10, 57, 76], and $1/N$ power-law [see Refs. 10, 16, 31, 57, 66, 69, 73–75] profiles. In order to evaluate the influence of these approximations of the mean flow, Nayfeh, Kaiser and Shaker[57] compared the attenuation rates that result from the use of five different approximations to the shape of the mean profile. Their results show that the attenuation rates from the various profiles can be correlated by using two scaling parameters: first, the shape factor[9] (ratio of displacement thickness to momentum thickness) of the approximate profile must be appropriate to the character of the actual flow; second, the displacement thickness, and not the boundary-layer thickness, should be used as the characteristic boundary-layer dimension. For example, Fig. 15, which presents the attenuation rate as a function of the boundary-layer thickness, demonstrates the substantial errors that can result from injudicious use of approximations to the mean flow. The improved correlation that results from use of the boundary-layer displacement thickness is shown in Fig. 16. The linear profile with slip at the wall was selected to have the same shape factor (1.29) as the $\frac{1}{7}$th power-law profile by proper choice of the slip velocity, and the results of these two profiles are in close agreement. The quadratic and Pohlhausen (p. 192, Ref. 9) profiles have nearly the same shape factors and produce nearly the same attenuation rates (the quarter sine and Blasius profiles, though not tested, are in the same range of shape factor, 2.5 to 2.66; any of these profiles should be suitable for calculating the effect of a laminar boundary layer); the widely used linear profile has a somewhat higher shape factor (3.0) and produces results that are slightly less useful in some instances. Thus, with proper scaling, the use of approximate mean-velocity profiles is suitable for prediction of the effect of shear layers on the propagation of sound.

Studies of the propagation of plane modes in rectangular ducts (see Refs. 10, 16, 31, 39, 54, 57, 69, 73, 74, 78, 79, 85), axially symmetric modes in circular[71,75] and annular[53,66,75] ducts, and higher-order circumferential modes in circular[80] and annular[40,76,77] ducts have all assessed the basic importance of the influence of velocity gradients in the mean flow. Two approaches have been used: studies of propagation in hard-wall ducts have determined the acoustic pressure profile in order to demonstrate the refraction of the sound; studies of propagation in lined ducts have determined the influence of the shear layers on the attenuation, a factor that depends upon the liner properties as well as on the amount of refraction.

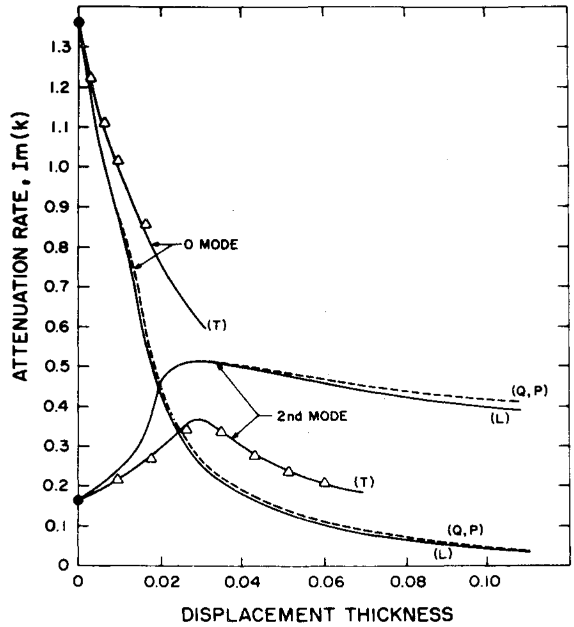

Fig. 16 Attenuation vs displacement thickness for several profile shapes; $M_c = -0.36$, $\omega = 5$, $R = 2$, $\omega_o = 56.3$, $h = 0.06748$; Δ—linear profile with slip at the wall; from Ref. 57.

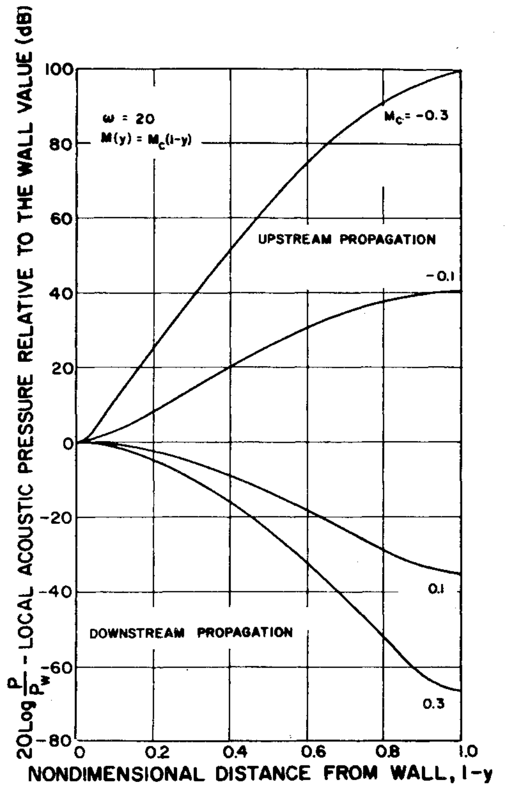

Fig. 17 Refraction of the fundamental mode in a rigid plane duct for $\omega = 20$; from Ref. 69.

In general, the shear layers refract the fundamental modes toward the wall for downstream propagation and away from the wall for upstream propagation (see Refs. 10, 16, 69, 73–76). This effect is clearly shown in Fig. 17, which presents the acoustic pressure profile of the lowest plane, symmetric mode for several values of the centerline Mach number and a nondimensional frequency of 20. For a Mach number of 0.3, these results give a centerline pressure which is approximately 65 db below the wall value for downstream propagation and 100 db greater than the wall value for upstream propagation. Note, however, that the shear layer is unrealistically large and that the frequency is very high, both of which serve to magnify the refraction.

It can also be seen in Fig. 17 that the refractive effect is increased by increasing the Mach number and is greater for upstream propagation. In addition, it is widely recognized that the refraction is greater for high frequency sound than it is for lower frequencies.[10,16,31,69,73] More precisely, the refraction is a function of the difference between the frequency and the cutoff frequency.[76,77]

Although the refraction of the higher modes is substantial,[53,69,73,76] the pressure profiles do not lend themselves to the simple interpretations given above. Shankar[74,75] has combined the first eleven modes to represent a plane wave at the duct entrance and then examined the pressure profile as the wave travelled downstream. At lower frequencies, the higher modes were cut off, and increasing frequencies produced greater refraction. However, at high frequencies and Mach numbers, the wave pattern was one of interference among the higher modes [recall that the hard-wall cutoff mode in uniform flow is $n\pi/2 = \omega/(1-M^2)^{1/2}$] rather than one of refraction.

In lined ducts, the channeling of the acoustic-pressure intensity by the shear profile as described above is expected to result in an increase in the attenuation rate for downstream propagation and a decrease in the attenuation rate for upstream propaga-

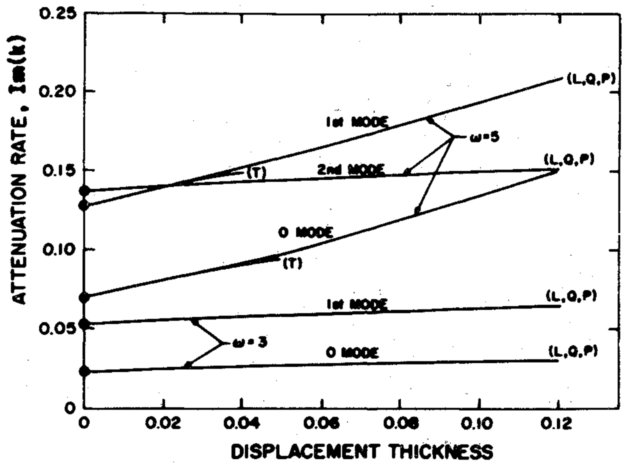

Fig. 18 Attenuation vs displacement thickness for $\omega = 3$ and $\omega = 5$ in a plane duct; $M_c = 0.36$, $R = 2$, $\omega_o = 56.3$, $h = 0.06748$; from Ref. 57.

tion. This anticipated trend can be found in the results of most studies of the effect of shear flow in lined ducts (see Refs. 31, 53, 54, 57, 71, 76, 77, 79, 80). For example, the fundamental modes in Figs. 16 and 18 follow the expected trend: increasing the boundary-layer thickness leads to an increase in the attenuation in downstream propagation and a decrease in upstream propagation. However, exceptions to this trend have been noted in the higher modes (see, for example, Refs. 57, 71); Fig. 16 includes an example of such an exception. In addition, Savkar[54] obtained results in a certain Mach number range that were opposite to the expected trend for downstream propagation of the fundamental mode; however, in this case the variation may well be within the range of computational error (see Sec. IV-B, 1d).

The optimization of liner properties for upstream sound propagation has been discussed by Mariano,[86] who concluded that the potential loss of attenuation due to refraction of the sound away from the walls can be cancelled to a large degree by a proper selection of the liner properties.

The importance of examining the higher modes has been emphasized in the studies by Eversman,[71] Mariano,[79] and Ko[80] as well as Shankar.[74,75] Because the fundamental mode need not be the least attenuated, as demonstrated in Fig. 16, and because the higher modes do not always follow the expected trends, as discussed above, conclusions based on the behavior of just the fundamental mode can be erroneous.

The effect of the shear layer on downstream-propagating waves is usually much smaller than the effect on upstream propagating waves [see Refs. 10, 57, 71, 76, 77, 79, 80 and Fig.s 16 and 18]. The influence of the shear layer on the attenuation rate usually increases with increasing frequency—as shown in Fig. 18—due to the increased refraction at higher frequencies that was cited earlier. However, in some studies[79,80] the effect of the shear layer on the attenuation has reached a maximum and then decreased as the frequency was increased to very large values. This is a consequence of the use of Eq. (49) to describe the liner impedance: as $\omega h \to \pi$, Eq. (49) predicts a rigid wall.

With due regard to the exceptions noted above, the results of the computations cited above show that the effect of the velocity gradients in the mean flow act in opposition to the convective influence discussed in Sec. IV-A. Whereas, in downstream propagation, the gross motion of the fluid tends to increase the speed of propagation of the acoustic wave thereby decreasing its attenuation rate, the velocity gradients in the mean-flow boundary layer tend to refract the acoustic wave toward the wall thereby increasing the effectiveness of the liner and increasing the attenuation rate. For upstream propagation these effects are reversed. Also the refraction increases with increasing frequency. These trends have been measured experimentally, and are clearly shown by the data of Tack and Lambert[31] depicted in Fig. 19. The attenuation of the low frequency signal, 130 cps, follows closely the convective trend described in Sec. IV-A, indicating very little refractive effect of the shear layer on long wavelength signals. However, the refraction of the signal increases as the frequency increases, and at 2060 cps the attenuation is nearly flat over the experimental range of flow velocities, indicating nearly equal convective and refractive effects.

Direct comparisons of theoretical predictions and experimental measurements of attenuation in duct facilities have been presented by a number of investigators (see Refs. 39, 79, 80, 87–91). For such comparisons, it is desirable to match the theoretical pressure profile at an initial station to an experimentally measured profile. Since this data was not available in some instances, a number of approximations have been introduced for the modal distributions in the theoretical studies. The theoretical calculations of Mariano[39,79] and of Ko[80] contained an equal amplitude assumption for the modal energy distribution. In light of the basic importance of this assumption, the theory and experiment exhibited reasonable agreement. Both authors noted the critical need for a better understanding of modal distribution within ducts. Feder and Dean[87] investigated several assumptions for the modal distribution: all energy propagates in the least attenuated mode; all propagating modes initially have equal energy; and all propagating modes initially have equal amplitude. Plumblee[88] found that an assumption of constant sound pressure in the radial direction at the liner entrance closely approximated his experimental data for frequencies below 1620 Hz.

The work of Plumblee, Dean, and co-workers[88–91] has provided conclusive evidence of good agreement between experimental observation and theoretical predictions both for individual modes and combinations of modes. The key element

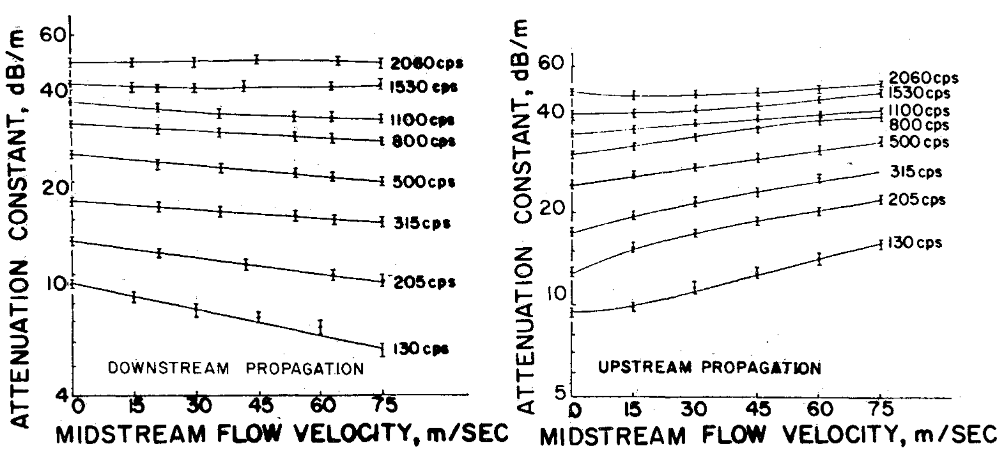

Fig. 19 Measured values of attenuation as a function of the centerline velocity; from Ref. 31.

in making such comparisons is the use of *in situ* measured values of liner impedance. The remaining discrepancies between experiment and theory appear to be a consequence of spatial variations in the liner properties due to inhomogeneities arising from the manufacturing process (these points are also discussed in the review article by Doak[92]).

Finally, it is noted that the mean flow in annular ducts may have a swirl component, i.e., a θ-component. The governing equations for acoustic propagation through such a flow have been developed by Kapur and Mungur,[93] but the influence of the swirl component of the mean flow has not been evaluated numerically.

C. Acoustic Boundary Layers

The solutions discussed above are all based on an assumption that the acoustic disturbance is inviscid and non-heat-conducting. The only effect of viscosity that has been included is an indirect one, the refractive effect of the velocity gradients in the mean flow. Because the inviscid, non-heat-conducting solutions do not satisfy the no-slip boundary condition, Eq. (58b), or the constant-temperature boundary condition, Eq. (58c), they are not valid in narrow regions near the duct walls, regions which we will call the acoustic boundary layers.

The existence of the acoustic boundary layer has long been recognized, with the earliest estimates of the influence of viscosity and heat conduction on the attenuation of plane waves propagating in rigid circular ducts being due to Kirchhoff and to Rayleigh.[94] Experimental tests of this result, extension to higher modes in both circular and rectangular ducts, and alternate formulations of the problem followed, with considerable discussion appearing in the literature of the 1950s (see, for example, Refs. 95–98). In all cases, these studies considered no mean flow within the duct.

The solution for the case of nonzero mean flow has been obtained by Nayfeh[99] using the method of composite expansions (see, for example, Sec. 4.2 of Ref. 17). In this approach, the acoustic disturbance is represented as the sum of the usual inviscid disturbance plus a viscous portion that is small everywhere except in a small layer, δ_a, near the wall. Taking $\delta_a = [2/Re\,\rho_o(1)\omega]^{1/2} = (2\tilde{\mu}_w/\tilde{\rho}\tilde{\omega}\tilde{d}_o{}^2)^{1/2}$, where the tilde indicates a dimensional quantity, and assuming that the mean-flow boundary layer is large compared with the acoustic boundary layer, Nayfeh showed that the effect of the acoustic boundary layer was to modify the wall boundary condition for the inviscid acoustic disturbance such that

$$dp(1)/dy = [\omega i p(1)/c_w]\beta_m$$

where

$$\beta_m = \frac{\beta + \delta_a \dfrac{1-i}{2\omega} c_w \left[k^2 + \dfrac{(\gamma-1)\omega^2}{(Pr)^{1/2} T_o(1)} \right]}{1 + i\delta_a \dfrac{1-i}{2\omega} \left[k u_o'(1) + \dfrac{T_o'(1)\omega}{(Pr)^{1/2} T_o(1)} \right]} \tag{95}$$

is an effective specific acoustic admittance.

Thus, even in a hard-walled duct, the acoustic boundary layer produces an effective admittance that is a function of the acoustic boundary-layer thickness, the wave number and frequency of the waves, and the mean velocity and temperature gradients at the wall. Numerical evaluation of the significance of the acoustic boundary layer has not been accomplished for cases with shear flow. However, for the case of no mean flow, the reactive component of Eq. (95) produces a dispersion that has been shown by Pestorius and Blackstock[100] to have a strong effect on the wave form of weak shocks propagating in rigid tubes.

The basic assumption that the acoustic boundary layer is small compared with the mean boundary layer is reiterated at this point. If the two layers are the same order, then it is necessary to return to Eqs. (16–20) for an evaluation of the viscous and heat-conduction influences on the acoustic wave. For the sake of illustration, if we assume a laminar, uniform-temperature mean flow, the boundary-layer thickness on a flat plate is $\delta = 5.0(x/R_e M_c)^{1/2}$, where x is the distance from the duct entrance (cf p. 130, Ref. 9). Thus

$$\frac{\delta_a}{\delta} = \frac{1}{5}\left(\frac{2M_c}{\omega x}\right)^{1/2}$$

and the ratio of the boundary-layer thicknesses need not be small.

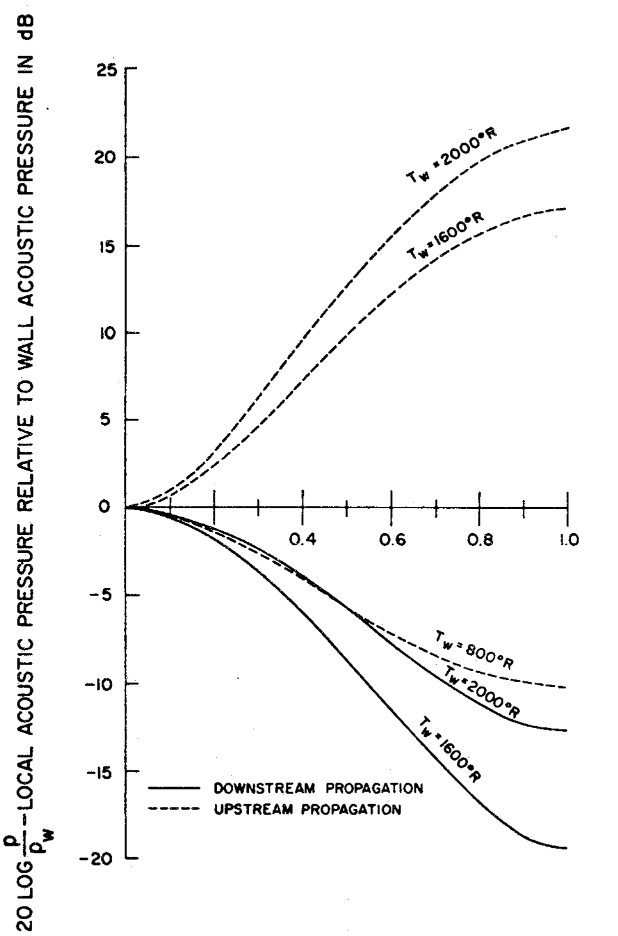

Fig. 20 Variation of sound level with distance from the wall for the lowest mode; from Ref. 104.

V. Effect of Temperature Gradients

Except for the work of Mungur and Tree,[101] Kapur and Mungur,[102,93] Kapur, Cummings and Mungur,[103] Nayfeh[99] and Nayfeh and Sun,[104] all the existing investigations of sound transmission and attenuation in ducts take into account mean velocity gradients but neglect mean temperature gradients.

Kapur, Cummings, and Mungur[103] analyzed the wave propagation in a combustion can with no mean flow, taking into account axial temperature and density gradients. They found that their solution was very sensitive to the acoustic transfer impedance of the system at the burner.

Mungur and Tree[101] derived an equation describing the acoustic pressure, taking into account both the mean velocity and temperature gradients, but presented numerical results only for the case of a rigid wall and no mean flow. Their results show that the temperature gradients have refractive effects similar to those for sheared mean flow. Moreover, the temperature gradients result in a contraction of the transverse wavelengths of some of the modes. Kapur and Mungur[102] investigated the interaction of boundary layers in the presence of transverse temperature gradients in a rectangular duct. No numerical results were presented.

Using the method of composite expansions (see, for example, Sec. 4.2 of Ref. 17), Nayfeh[99] found that the effect of the acoustic boundary layer is to modify the specific wall admittance. The modified admittance β_m depends on both the transverse velocity and temperature gradients, as shown in Eq. (95).

Nayfeh and Sun[104] evaluated numerically the effects of transverse temperature gradients in two-dimensional ducts carying mean flow. To discuss their results, it is more convenient to use the centerline temperature T_c and mean velocity u_c instead of the ambient values in making the variables dimensionless. Thus, Eq. (21) becomes

$$\frac{d^2p}{dy^2} - \left[\frac{2ku_o'}{u_o k-\omega} - \frac{T_o'}{T_o}\right]\frac{dp}{dy} + \left[\frac{M_c^2(u_o k-\omega)^2}{T_o} - k^2\right]p = 0 \qquad (96)$$

where M_c is the centerline Mach number. For a flat plate, the mean-temperature profile is related to the mean-velocity profile by (see, for example, pp. 339–346 of Ref. 9)

$$T_o(y) = 1+(T_w-1)[1-|u_o(y)|]+\tfrac{1}{2}(\gamma-1)r \times M_c^2|u_o(y)|[1-|u_o(y)|] \qquad (97)$$

where the recovery factor r can be adjusted to fit the experimental data. It was taken to be unity in the calculations. The mean-velocity profile is assumed to be uniform except in thin boundary layers where it is linear, that is,

$$u_o(y) = \pm 1 \qquad \text{for} \qquad 0 \leqq y \leqq 1-\delta \qquad (98a)$$

$$u_o(y) = \pm(1-y)/\delta \qquad \text{for} \qquad 1-\delta \leqq y \leqq 1 \qquad (98b)$$

where the positive and negative signs are used to investigate downstream and upstream propagation, respectively. The calculations were performed using the forward-integration procedure described in Sec. IVB for the case of symmetric modes; that is, for

$$dp/dy = 0 \qquad \text{at} \qquad y = 0 \qquad (99)$$

Figure 20 shows the variation of the sound level in the lowest mode with the wall temperature and with the distance from the wall for the case of a hard-walled duct and the conditions: $M_c = \pm 0.36$, $\delta = 0.06$, $\gamma = 1.4$, $T_a = 519°R$, and $T_c = 2000°R$. Figure 20 shows that cooling the wall directs the sound toward the walls for both upstream and downstream propagation.

For downstream propagation and soft walls with $\omega_o = 56.3$, and $h = 0.06748$, Fig. 21 shows that cooling the duct walls leads to a shift in the peak attenuation rate to a lower dimensionless flow resistance. The peak value may increase or decrease with wall cooling depending on the frequency. Moreover, their numerical results show that the wave number is insensitive to temperature gradients but the attenuation rate increases as the wall is cooled.

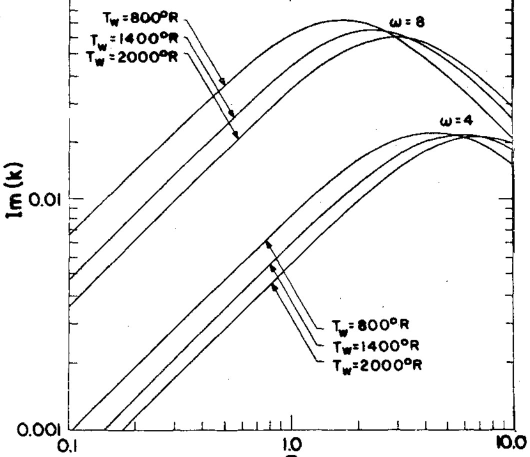

Fig. 21 Effect of wall temperature and dimensionless flow resistance on the attenuation rates of the lowest two modes for $T_c = 2000°R$ and downstream propagation; from Ref. 104.

For upstream propagation their results show that heating the duct walls leads to a decrease in the attenuation rate. However, the rate of decrease of the attenuation rate with wall temperature decreases as the mode number increases. Moreover, the peak attenuation rate of the lowest mode decreases and shifts to a higher dimensionless flow resistance as the wall temperature increases. No numerical results are yet available for circular and annular ducts.

VI. Ducts with Variable Cross Sections

There are many physical situations which require the prediction of the wave propagation and attenuation in ducts with varying cross sections with or without mean flows. These situations include horns, loudspeakers, central air conditioning and heating installations, high speed wind tunnels, aircraft-engine duct systems, and rocket nozzles. We start our discussion with the case of no mean flows and follow it with the case of mean flows in Sec. VIB.

A. Case of No Mean Flow

A number of approaches have been developed to analyze the wave propagation in ducts with variable cross sections without mean flows. These approaches include expansions for low frequencies, variational methods, approximation of the duct by series of stepped uniform sections, and the method of multiple scales. These approaches are discussed in order below.

1) *Expansions for low frequencies*

Webster[105] integrated the linearized acoustic equations (10–12) with ρ_o constant over the duct cross section and obtained

$$\frac{1}{S}\frac{\partial}{\partial x}\left(S\frac{\partial p_1}{\partial x}\right) = \frac{1}{c^2}\frac{\partial^2 p_1}{\partial t^2} \qquad (100)$$

where S is the cross-sectional area of the duct. This equation is referred to as Webster's horn equation. It can also be derived from the quasi-one-dimensional, incompressible equations of motion by expanding the flow variables about the uniform pressure p_o and density ρ_o.

Closed-form solutions have been found for Eq. (100) for conical, exponential, and catenoidal horns. Extensive studies of Webster's equation have appeared in the literature (see, for example, Ref. 106).

Puebe and Chasseriaux[107] carried out an expansion of the acoustic equations in powers of d_o/λ, where λ is the wave length. The first term in their expansion corresponds to Webster's equation.

Note that Webster's equation describes only the lowest (zeroth mode) of sound propagation. To determine the other modes, one needs to use one of the techniques described in the following sections.

2) *Variational methods*

There are two variants of this method. In the first approach (Rayleigh-Ritz procedure), which is commonly used by solid mechanicians, a functional is formed such that its first variation gives the acoustic equation and the appropriate boundary conditions. One then assumes a solution with undetermined coefficients and determines the equations describing these coefficients by minimizing the functional. Such an approach is being pursued by Beckemeyer and Eversman[108] for ducts with or without flow.

In the second approach (Galerkin procedure), one assumes a solution with undetermined coefficients and determines the equations describing the coefficients by substituting the assumed solution into the governing equations of motion and boundary conditions and minimizing, in some sense, the error. Such an approach is most commonly employed in solid mechanics and in electromagnetic wave theory. Stevenson[109] applied this technique to the problem of wave propagation in hard-walled ducts. He assumed that the acoustic velocity potential has the form

$$\phi = \Sigma A_{mn}(x)\psi_{mn}(y, z;\ x)\exp(-i\omega t) \tag{101}$$

where ψ_{mn} are the orthonormal characteristic modes for the wave propagation in a uniform duct having a cross section the same as the local cross section of the non-uniform duct. The corresponding wave number is denoted by k_{mn}. For a rectangular duct with half widths $b(x)$ and $d(x)$,

$$\psi_{mn} = \frac{2}{(bd)^{1/2}}\cos\frac{n\pi y}{b}\cos\frac{m\pi z}{d} \tag{102a}$$

$$k_{mn}{}^2 = \omega^2 - \frac{n^2\pi^2}{b^2} - \frac{m^2\pi^2}{d^2} \tag{102b}$$

Substituting Eq. (101) into the governing equation and boundary conditions and using the orthonormality of the ψs, he arrived at coupled ordinary differential equations of the form

$$\frac{d^2A_{mn}}{dx^2} + k_{mn}{}^2A_{mn} = F(A_{sr}) \tag{103}$$

where F is a function of all the A's.

By neglecting the interaction between the different modes (i.e., $F = 0$), Stevenson solved the resulting uncoupled equations by using the *WKB* method (see, for example, Sec. 7.1.3 of Ref. 17) and obtained

$$A_{mn} = \frac{a_{mn}}{(k_{mn})^{1/2}}\exp(i \textstyle\int k_{mn}\,dx) \tag{104}$$

where a_{mn} is a constant. This solution breaks down if k_{mn} vanishes at some axial location in the duct. Using a turning-point analysis (see Sec. 7.3.2 of Ref. 17), one can express the solutions of the uncoupled Eq. (103) in terms of the Airy function of the first kind. Thus, if $k_{mn} = 0$ at an axial location x_o, the mode (m, n) consists of a standing wave on one side of x_o and an exponentially attenuated wave on the other side.

3) *Approximations of ducts by stepped uniform sections*

The basis of this approach is the solution obtained by Miles[110] for the reflection and refraction of sound as it propagates past a single discontinuity (Fig. 22). He imposed the conditions of continuity of pressure and velocity over the region $0 \leqq r \leqq d_1$ and vanishing of velocity over the region $d_1 \leqq r \leqq d_2$. The result is an infinite series of coupled algebraic equations for an infinite number of coefficients. This infinite series must be truncated after a finite number of terms and the accuracy of the resulting solution deteriorates as the ratio d_2/d_1 increases.

Zorumski and Clark[111] and Lansing and Zorumski[112] analyzed the effect of a continuous variation in the wall admittance of a duct with uniform cross section by approximating the duct by a series of sections, each with a different admittance. They matched the pressure and velocity at all interfaces of the different sections. Alfredson[113] extended the method of Zorumski and Clark to include variations in the cross sections.

4) *Slowly-varying cross sections*

Nayfeh and Telionis[114] used the method of multiple scales (see Chap. 6 of Ref. 17) to determine the propagation of a wave packet in rectangular and circular ducts with slowly varying cross sections and slowly varying wall admittance. They assumed the acoustic velocity potential to have the form

$$\Phi(x_1, T_1, y, z;\ \varepsilon)\exp(i\phi)$$

where $x_1 = \varepsilon x$ and $T_1 = \varepsilon t$, with ε a small parameter the order of the maximum slope of the wall and

$$\partial\phi/\partial t = -\omega(x_1, T_1) \quad \text{and} \quad \partial\phi/\partial x = k(x_1, T_1) \tag{105}$$

with ω the frequency and k the complex wave number. Expanding Φ in powers of ε according to

$$\Phi = \Phi_o(x_1, T_1, y, z) + \varepsilon\Phi_1(x_1, T_1, y, z) + \ldots, \tag{106}$$

substituting into the wave equation and the boundary conditions, and equating coefficients of like powers of ε, they obtained problems for Φ_o and Φ_1.

The solution of the first-order problem is

$$\Phi_o = A(x_1, T_1)\psi(y, z;\ x_1) \tag{107}$$

where ψ is the characteristic mode obtained by assuming that the cross section is uniform. $A(x_1, T_1)$ is still an undetermined function. The second-order problem for Φ_1 is inhomogeneous, and it has a solution if, and only if, a solvability condition is satisfied. This condition yields an equation for A of the form

$$\partial E/\partial T_1 + \partial/\partial x_1[(d\omega/dk)E] = 0 \tag{108}$$

where for two-dimensional ducts

$$E = \frac{A^2 d}{4}\left(\omega^2 + \frac{k^2\sin 2k_y d}{2k_y d}\right) \tag{109}$$

$d(x_1)$ is the duct half width and k_y is a solution of

$$k_y \tan k_y d = -i\omega\beta \tag{110}$$

For rigid walls, $k_y = n\pi/d$, E is the acoustic energy flux and $d\omega/dk$ is the group velocity.

For a monochromatic wave ($\partial\omega/\partial T_1 = \partial A/\partial T_1 = 0$), Eq. (108) integrates into

$$A^2 k\left(d + \frac{\sin 2k_y d}{2k_y}\right) = \text{const} \tag{111}$$

Note that this solution is invalid at any axial location x_o where $k \approx 0$. In such cases, the exponential variation of Φ_1 with x must be replaced by that of an Airy function. The modified solution shows that such a mode consists of a standing wave on one side of x_o and an exponentially attenuated wave on the other side. For the case of hard-walled ducts, the solution of Nayfeh and Telionis is equivalent to that of Stevenson for slowly varying ducts.

5) *Sinusoidally varying walls*

Isakovitch,[115] Samuels,[116] and Salant[117] obtained perturbation solutions for wave propagation in ducts whose rigid walls have sinusoidal variations of small amplitude. Under certain conditions, their solutions predict unbounded disturbances from the small wall variations; hence, the basic perturbation expansion is invalid at these resonant conditions. They tabulated the resonant frequencies from numerical solutions but did not examine the nature of the wave propagation near resonance. Nayfeh[118] pointed out that resonance occurs whenever the wave number of the wall variations, k_w, equals the sum or difference of the wave numbers, k_m and k_n, of any two acoustic modes, and he obtained the solution for the wave propagation near resonance. His solution shows that only the resonant case $k_w \simeq k_n - k_m$ occurs in traveling waves, but both resonances, $k_w \simeq k_n \pm k_m$, can occur in standing waves. Further, the solution shows that the amplitudes of both modes are bounded and that the two modes interact such that one mode cannot be excited without strongly exciting the other.

B. The Case of Mean Flow

Large and co-workers[119] found experimentally that sizable attenuation of acoustic waves is possible in a duct with an inlet throat if the mean flow Mach number is 0.8–0.9. Chestnut and Clark[120] investigated experimentally the effect of inlet waveguide vanes (cambered, uncambered, translating and rotating) on the reduction of noise in jet engines. A pure tone of 500 Hz

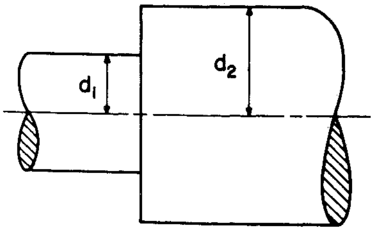

Fig. 22 Geometry of single discontinuity.

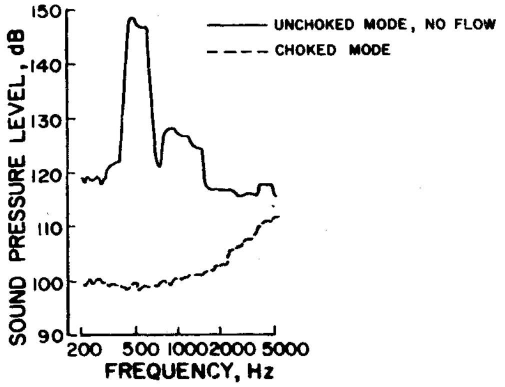

Fig. 23 Noise spectra of stationary, uncambered inlet guide vane; from Ref. 120.

was directed against the mean flow and through the throat. Figure 23 shows a sample of their results for an uncambered inlet waveguide vane. Note that the pure tone and all its harmonics were completely attenuated and the broad-band noise was considerably reduced. They found that the fundamental mode may be transmitted through the throat with little attenuation even if the mean flow is fully choked. They attributed this phenomenon to sound transmission through the mean boundary layer.

These experimental discoveries motivated several theoretical investigations of the wave propagation in ducts of varying cross sections with mean flows. Direct application of purely numerical techniques to the acoustic equations are in their infancy; the first attempts[121,122] have examined simplified flow cases to develop the necessary numerical techniques. King and Karamcheti[121] applied the method of characteristics to solve the quasi-one-dimensional acoustic equations in the x-t plane. Baumeister and Rice[122] used a finite-difference method to examine harmonic waves in a two-dimensional uniform duct with uniform flow. However, most studies have employed an analytical technique or approximation, frequently in conjunction with a numerical solution. These investigations are discussed below in order of increasing complexity of their approximations for the mean flow: one-dimensional flow; one-dimensional flow with a normal velocity component, and two-dimensional flow.

1) *Quasi-one-dimensional flows*

Most of the work done on the wave propagation in slowly-varying ducts with mean flows is based on the hypothesis that both the mean flow and the acoustic wave are quasi-one-dimensional. Some of the approaches and results are discussed below.

a) Propagation of discontinuities: Whitham[123] and Rudinger[124] treated the propagation of shock waves in ducts with varying cross sections, while Powell[125] used a multiple reflection method to develop a one-dimensional treatment of the propagation of a pressure pulse through a channel with a variable cross section and carrying a compressible flow. Assuming that the whole incident wave is transmitted, he concludes that

$$p_1{}^2 S(1+M)/\rho_o c_o = \text{const} \tag{112}$$

where p_1 is the rms pressure increment. Thus one expects the wave to increase on encountering a decreasing passage area at low mean velocities. At Mach numbers exceeding 0.4, he found that the wave strength decreases on encountering a decreasing passage area, in qualitative agreement with the experimental results of Refs. 119 and 120. Powell[126] also extended his multiple reflection method to sinusoidally varying pressure waves.

b) An exact solution: Eisenberg and Kao[127] analyzed the linear quasi-one-dimensional wave propagation in a duct with variable cross section and carrying quasi-one-dimensional mean flow. The governing equations were transformed into a pair of uncoupled second-order ordinary differential equations with variable coefficients. By choosing an appropriate, semi-infinite, divergent duct from the sonic throat, they were able to reduce these equations to equations with constant coefficients. Their results show that the wave amplitude may increase or decrease in a converging channel depending on the mean flow Mach number and the wave frequency. Their solution exhibits standing-wave characteristics with wave amplitude approaching infinity as the throat is approached. For a general duct, numerical techniques can be used to solve the variable-coefficient equations.

c) Numerical methods: Solutions of the one-dimensional acoustic equations with variable coefficients have been obtained by Davis and Johnson[128] and by Kooker and Zinn.[129] Davis and Johnson used a forward-integration, "shooting" technique to obtain solutions for traveling waves in several duct-nozzle configurations. Kooker and Zinn used a relaxation technique to solve for standing waves in a combustion-chamber choked-nozzle configuration.

An alternate approach in which the duct is approximated by a series of cylindrical and conical sections has been developed by Hogge and Ritzi.[130] In this analysis, only the mean flow is assumed to be one-dimensional; all acoustic modes are included. Analytic solutions in each section (for conical sections an asymptotic solution for small cone angles is used) are matched at the approximate interfaces between sections. Since the end surfaces of the conical sections are spherical rather than planar, the interfaces between sections do not match exactly and some error is thus introduced.

d) WKB approximation: Huerre and Karamcheti[131] analyzed the propagation of the lowest acoustic mode in a duct with variable cross section carrying quasi-one-dimensional, compressible mean flow. Assuming each flow quantity to be the sum of a steady part and an acoustic part, they derived the equations describing the acoustic parts. These equations were combined to yield the following equation for the acoustic velocity potential

$$\frac{D^2\Phi}{Dt^2} = c_o{}^2\frac{\partial^2\Phi}{\partial x^2} + \left[\frac{dh_o}{dx} + c_o{}^2\frac{d}{dx}(\log S)\right]\frac{\partial\Phi}{\partial x} + u_o\frac{d}{dx}(\log c_o{}^2)\frac{D\Phi}{Dt} \tag{113}$$

$$D/Dt = \partial/\partial t + u_o(x)(\partial/\partial x)$$

which is a generalization of Webster's horn equation (100) to the case of compressible mean flows.

Huerre and Karamcheti sought an approximate solution to Eq. (113) for short waves (ray acoustics) by letting

$$\Phi(x,t) = [\psi_o(x) + \varepsilon\psi_1(x) + \ldots]\exp[i\omega t - i\omega\theta(x)] \tag{114}$$

where

$$\varepsilon = -i/\omega \ll 1$$

Substituting Eq. (114) into Eq. (113) and equating coefficients of like powers of ε, they obtained the desired equations describing θ and ψ_n. Solving these equations and then determining the acoustic pressure, they obtained the following equation for the pressure amplitude

$$A \propto \frac{1}{M(x)\pm 1}\left(\frac{\rho_o(x)c_o(x)}{S(x)}\right)^{1/2} \tag{115}$$

which apart from the factor $(M\pm 1)^{1/2}$ is equivalent to Eq. (112), the equation obtained by Powell.[125]

2) *Flows with a normal velocity component*

Tam[132] used the Born approximation (see, for example, Sec. 7.4.1 of Ref. 17) to determine the backscattering of a spinning acoustic-wave mode in a circular duct with variable cross section when it is incident in the upstream direction on a throat or constriction in the duct. He assumed that the radius of the duct near the throat varied according to

$$r = 1 - \varepsilon\alpha(x), \qquad \varepsilon \ll 1 \tag{116}$$

and he modeled the mean flow by

$$u_o(r,x) \approx U(0,x) \qquad v_o(r,x) \approx \varepsilon U(0,x) r(d\alpha/dx) \tag{117}$$

Thus, he included the effect of a small normal velocity component but neglected the refractive effect of the boundary layer. He assumed the total wave to consist of an incident and a scattered part and used the Born approximation to determine the equations describing the scattered part, which he then solved by using Fourier transforms.

His results show that the backscattering is unimportant for axial Mach numbers below 0.4. However, a substantial attenuation of wave energy is possible for an axial flow Mach number of about 0.6 and throats of reasonable area reduction, in qualitative agreement with the experimental observations.

3) *Flows with transverse velocity gradients*

Nayfeh, Telionis and Lekoudis[133] used the method of multiple scales (Chap. 6 of Ref. 17) to analyze the propagation of all acoustic modes in a two-dimensional duct with a slowly varying cross section that carries an incompressible, sheared mean flow. Extension of the analysis to annular ducts has been accomplished by Nayfeh, Kaiser, and Telionis.[134] In the two-dimensional case the mean flow is given by Eq. (28) with constant ρ_o, T_o, and p_o and the acoustic wave is given by Eqs. (29). The expansions

$$p = F_o(y;\ x_1) + \varepsilon F_1(y;\ x_1) + \ldots \tag{118}$$

$$u = G_o(y;\ x_1) + \varepsilon G_1(y;\ x_1) + \ldots \tag{119}$$

$$v = H_o(y;\ x_1) + \varepsilon H_1(y;\ x_1) + \ldots \tag{120}$$

are substituted into Eqs. (31–33) with constant ρ_o, T_o, and p_o and into the boundary conditions, the equations are expanded for small ε, and the equations describing F_n, G_n and H_n are obtained by equating coefficients of like powers of ε. G_n and H_n are eliminated to yield a homogeneous, ordinary differential equation, with homogeneous boundary conditions, for $F_o(y;\ x_1)$ and to yield an inhomogeneous problem for $F_1(y;\ x_1)$. The problem for $F_o(y;\ x_1)$ is the same as that for acoustic propagation in parallel ducts, Eqs. (22) and (72), except that x_1 appears as a parameter in the duct dimension $d(x_1)$ and in the mean-flow component $u_o(y;\ x_1)$. Hence the solution has the form

$$F_o(y;\ x_1) = A(x_1)\psi(y;\ x_1) \tag{121}$$

where $\psi(y;\ x_1)$ is the eigenfunction calculated at each station of the duct as if the flow and duct walls were parallel. The corresponding eigenvalue is denoted by k_o. To determine $A(x_1)$, a requirement that the asymptotic expansion, Eqs. (118–121), be uniformly valid to $0(\varepsilon)$ is imposed. That is, a solvability condition is imposed on the inhomogeneous equations governing F_1. This condition yields an equation of the form

$$f(x_1)(dA/dx_1) + g(x_1)A = 0 \tag{122}$$

where $f(x_1)$ and $g(x_1)$ are obtained numerically from integrals across the duct width of ψ, u_o, v_o, k_o, and their derivatives.

Equation (122) has the solution

$$A(x_1) = A_o \exp\left[i\int k_1(x_1)\,dx_1\right] = A_o \exp\left[\varepsilon i\int k_1(x_1)\,dx\right] \tag{123}$$

where $k_1(x_1) = ig(x_1)/f(x_1)$ and A_o is a constant to be determined from initial conditions.

The final form of the acoustic pressure disturbance is found, by combining Eqs. (29), (30), (118), (121) and (123):

$$p_1(x,y,t) = A_o\psi(y;x_1)\exp\left[i\int(k_o+\varepsilon k_1)\,dx - i\omega t\right] + 0(\varepsilon) \tag{124}$$

The equivalent form for annular ducts is

$$p_1(x,r,\theta,t) = A_o\psi(r;x_1)\exp\left[i\int(k_o+\varepsilon k_1)\,dx + im\theta - i\omega t\right] + 0(\varepsilon) \tag{125}$$

Without $k_1(x_1)$, the solutions represented by Eqs. (124) and (125) are quasi-parallel approximations predicting an attenuation rate $\alpha_o = Im(k_o)$. The function $k_1(x_1)$ contains the effects of the nonparallel walls and of the axial derivatives of the mean flow. The net attenuation rate is then given by $\alpha_o + \varepsilon\alpha_1 = Im(k_o + \varepsilon k_1)$.

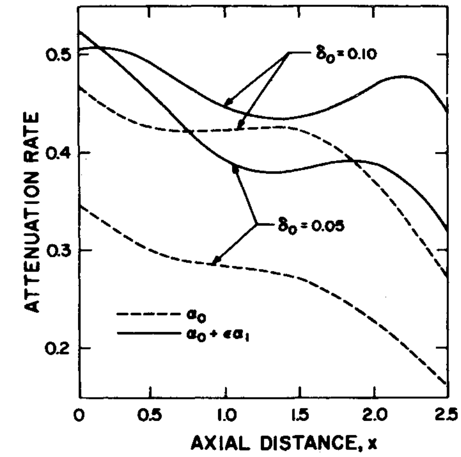

Fig. 24 Effect of the mean boundary-layer thickness on the attenuation of the (0, 0) mode for $\omega = 30$; $R = 2$, $\omega_o = 100$, $h = 0.05$; $\varepsilon = 0.214$; from Ref. 134.

A sample result is presented in Fig. 24 for downstream propagation of the fundamental mode in a slowly-diverging, lined, annular duct with a growing boundary layer. Calculations for two different values of δ_o, the boundary-layer thickness at the initial station $x = 0$, are presented. As expected from the results of numerous parallel-flow studies, (see Sec. IV-B2), the quasi-parallel approximation predicts a lower attenuation (proportional to the area under the curve) when the boundary layer is thinner. However, it can be seen that the effects of the axial gradients are much larger for the thinner boundary layer. Thus, for this particular case, the thicker boundary layer does not produce a large increase in the attenuation, a fact that a quasi-parallel analysis would not reveal.

VII. Nonlinear Effects

Measured data in typical jet engines indicate that the sound pressure level involved may be in excess of 160 db which corresponds to a pressure fluctuation of the order of 0.01 atm. At these levels, the nonlinear effects play an important role in the attenuation of the sound. These nonlinear effects can be classified into two types: the nonlinearity of the gas itself and the nonlinearity of the acoustic properties of the lining material. Although the gas nonlinearity is significant at sound pressure levels exceeding 160 db, the material nonlinearity (especially, perforated plates) may be significant at sound pressure levels above 130 db. In this section, we discuss the nonlinear effects and the approaches used to predict them.

Most of the studies of the nonlinear effects of the gas have been based on an irrotational, inviscid, compressible wave propagating in a medium at rest with uniform density ρ_o and pressure p_o. Thus, the velocity of the wave can be derived from a potential function $\Phi(r,t)$ which is given by (see, for example, Ref. 135)

$$c^2\nabla^2\Phi - \Phi_{tt} = 2\nabla\Phi\cdot\nabla\Phi_t + \tfrac{1}{2}(\nabla\Phi\cdot\nabla)(\nabla\Phi)^2 \tag{126}$$

where, for a perfect gas,

$$c^2 = (1-\gamma)[\Phi_t + \tfrac{1}{2}(\nabla\Phi)^2] + 1 \tag{127}$$

$$\gamma p = \rho^\gamma = \rho c^2 \tag{128}$$

where p and ρ are the dimensionless pressure and density. In Eqs. (126–128), distances, velocities, time, density, and pressure were made dimensionless using the reference quantities d_o, c_o, d_o/c_o, ρ_o, and $\rho_o c_o^2$, respectively, where d_o is a characteristic length of the duct cross section and c_o is the speed of sound in the undisturbed medium.

Hard-walled ducts are discussed in the next section, while soft-walled ducts are discussed in Sec. VII-B.

A. Hard-Walled Ducts

1) *Plane waves*

Most of the work done on nonlinear wave propagation in hard-walled ducts deals with plane waves. Fay[136] obtained a Fourier series solution, valid in the far field, for the one-dimensional wave equation taking into account the effects of gas compressibility and viscosity. Fubini[137] obtained a solution, valid in the near field, for the one-dimensional, isentropic wave equation in terms of Bessel functions. Blackstock[138] used the weak shock theory to obtain a general solution which is valid in the near and far fields as well as the transition between them. Coppens[139] and Pestorius and Blackstock[100] determined the viscous and thermal dissipative effects on the nonlinear propagation of plane waves in hard-walled ducts.

2) *Higher modes*

Maslen and Moore[140] used the method of strained parameters (Sec. 3.1 of Ref. 17) to analyze strong transverse waves in a circular cylinder. They determined the effect of the amplitude on the frequency of oscillation. They also determined the dissipation effects of the acoustic boundary layer.

Burns[141] analyzed finite-amplitude waves in a hard-walled duct, taking into account dissipation. However, his expansion is not uniformly valid because it contains secular terms. Keller and Millman[142] used the method of strained parameters to determine the wave number shift for the symmetric dispersive modes in a hard-walled duct. They assumed expansions of the form

$$\Phi(x, y, z, t;\ \varepsilon) = \sum_{n=1}^{3} \varepsilon^n \Phi_n(kx-\omega t, y, z) + 0(\varepsilon^4) \tag{129}$$

$$p(x, y, z, t;\ \varepsilon) = p_o + \sum_{n=1}^{3} \varepsilon^n p_n(kx-\omega t, y, z) + 0(\varepsilon^4) \tag{130}$$

$$k = k_o + \tfrac{1}{2}\varepsilon^2 k_2 + 0(\varepsilon^3) \tag{131}$$

where the x axis coincides with the duct axis, Φ is the velocity potential, p_o is the undisturbed pressure which is assumed to be uniform, and ε is a small dimensionless parameter characterizing the amplitude of the wave. For a hard-walled duct, the boundary condition on the duct surface is

$$\partial\Phi/\partial n = 0 \qquad \text{on} \qquad \Gamma \tag{132}$$

where Γ is the duct cross-section perimeter. Substituting Eqs. (129–131) into Eqs. (126), (127) and (132) and equating coefficients of like powers of ε, they obtained problems describing Φ_n and p_n. The solution of the first-order problem was taken to consist of one mode; that is,

$$\Phi_1 = a\psi(y, z)\cos(kx-\omega t) \tag{133}$$

$$p_1 = -\rho_o \omega a \psi(y, z)\sin(kx-\omega t) \tag{134}$$

$$k_o^2 = \omega^2 - \kappa^2 \tag{135}$$

where a is an arbitrary constant and $\psi(y, z)$ is the eigenfunction corresponding to the eigenvalue κ of the problem

$$\partial^2\psi/\partial y^2 + \partial^2\psi/\partial z^2 + \kappa^2\psi = 0 \tag{136}$$

$$\partial\psi/\partial n = 0 \qquad \text{on} \qquad \Gamma \tag{137}$$

The second-order terms Φ_2 and p_2 were obtained by solving the second-order problem. Then, k_2 was determined from the third-order problem by using the solvability condition (elimination of secular terms in this case).

The expansion obtained by Keller and Millman is not valid near the cutoff frequencies. Keller[143] modified the expansion of Ref. 142 and determined the amplitude dependence of the cutoff frequencies of the symmetric modes.

Nayfeh[144] used the method of multiple scales to derive the following pair of partial differential equations describing the temporal and spatial modulation of the amplitudes and phase of all modes propagating in a hard-walled circular duct:

$$\omega\frac{\partial A}{\partial T_1} + k\frac{\partial A}{\partial X_1} = 0 \tag{138}$$

$$2i\left(\omega\frac{\partial A}{\partial T_2} + k\frac{\partial A}{\partial X_2}\right) - \frac{\partial^2 A}{\partial T_1{}^2} + \frac{\partial^2 A}{\partial X_1{}^2} = \Lambda A^2\bar{A} \tag{139}$$

where Λ is an interaction constant depending on the mode being considered,

$$A = \tfrac{1}{2}a\exp(i\beta) \tag{140}$$

and

$$T_n = \varepsilon^n t, \qquad X_n = \varepsilon^n x \tag{141}$$

with a and β being the amplitude and the phase.

Eliminating the derivatives with respect to X_1 from Eqs. (138) and (139) and rewriting the result in terms of the original variables leads to the following nonlinear Schrödinger equation:

$$\frac{\partial A}{\partial x} + k'\frac{\partial A}{\partial t} + \tfrac{1}{2}ik''\frac{\partial^2 A}{\partial t^2} = -\tfrac{1}{2}i\varepsilon^2\frac{\Lambda}{k}A^2\bar{A} \tag{142}$$

where

$$k' = dk/d\omega \qquad \text{and} \qquad k'' = d^2k/d\omega^2$$

Using this equation, Nayfeh determined an expression for monochromatic waves and then showed that these waves are stable. However, this expansion is not valid near the cutoff frequencies.

Eliminating the derivatives with respect to T_1 from Eqs. (138) and (139) and expressing the result in terms of the original variables, Nayfeh obtained the following nonlinear Schrödinger equation valid everywhere including the cutoff frequencies:

$$\partial A/\partial t + \omega'\,\partial A/\partial x - \tfrac{1}{2}i\omega''\,\partial^2 A/\partial x^2 = -\tfrac{1}{2}i\Lambda\omega^{-1}\varepsilon^2 A^2\bar{A}$$

where $\omega' = d\omega/dk$ and $\omega'' = d^2\omega/dk^2$. Using this equation, Nayfeh obtained an expansion for monochromatic waves from which he determined the amplitude dependence of the cutoff frequencies of all modes.

Peube and Chasseriaux[107] treated nonlinear wave propagation in hard-walled ducts with variable cross section. They proposed two perturbation expansions using as the small parameter the Mach number M and d_o/λ, where λ is the wave length. Thus, they assumed

$$\Phi(\mathbf{r}, t) = \sum_{n=0}^{\infty}\left(\frac{d_o}{\lambda^2}\right)^{2n}\Phi_n(\mathbf{r}, t) \tag{143}$$

or

$$\Phi(\mathbf{r}, t) = \sum_{n=0}^{\infty} M^n\Phi_n(\mathbf{r}, t) \tag{144}$$

Substituting either Eq. (143) or (144) into Eqs. (126), (127) and (132) and equating coefficients of like powers of d_o/λ or M, they obtained the appropriate equations and boundary conditions describing the Φ's. However, no solutions were obtained to assess the nonlinear effects.

B. Soft-Walled Ducts

As mentioned earlier, there are two types of nonlinearities: the nonlinear motion of the gas and the nonlinear lining acoustic properties. Zorumski and Parrott[145] and Kurze and Allen[78] found, experimentally, that the nonlinear effects tend to flatten and broaden the absorption vs frequency curve as shown in Fig. 25. At resonance, the high intensity level increases the resistance of the liner resulting in a lower attenuation. To quantify the nonlinear effects on the attenuation, a number of approaches have been devised. Some of these approaches are discussed below.

1) *Lowest mode*

Ingard[146,147] used the one-dimensional transmission line approximation to determine the nonlinear material effect on the attenuation of the lowest mode at low frequencies. Thus, the pressure was assumed to be uniform across the duct, and the rate of energy absorption per unit length of the boundary of the duct was expressed as $\beta p^2\Gamma$, where p is the rms value of the sound pressure. Since the energy flux through the duct is $p^2 S$, its rate of change along the duct must be equal to the energy absorbed by the liner; that is,

$$2S\,dp/dx = -\beta p\Gamma \tag{145}$$

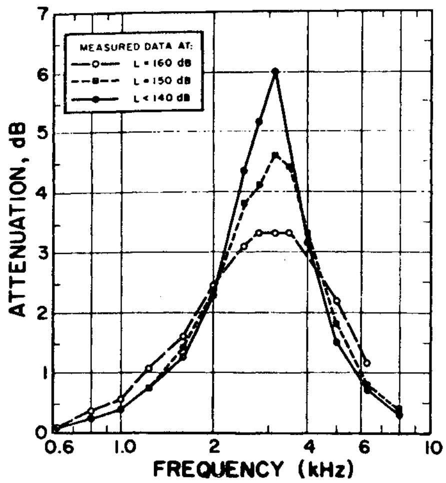

Fig. 25 Variation of attenuation over a distance d_o with frequency for several sound pressure levels, L; from Ref. 78.

Expressing β as a function of p, Ingard solved Eq. (145) to obtain

$$\int_{p_o}^{p} [dp/p\beta(p)] = -\Gamma x/2S \qquad (146)$$

where p_o is the sound pressure at $x = 0$.

To perform the integration in Eq. (146), the specific admittance must be specified. Following Ingard and Ising,[148] Ingard assumed that

$$z = R_o + 0.9 R_1 u_{\rm rms} + i\chi \qquad (147)$$

where $u_{\rm rms}$ is the rms face velocity of the fundamental frequency component. In Ref. 147, Ingard took $\chi = 0$ and $0.9R_1 u_{\rm rms} = p^{1/2}$, while in Ref. 148, he related $u_{\rm rms}$ to the incident rms sound pressure by

$$u_{\rm rms} = p_{\rm rms}/|z| \qquad (148)$$

Kurze and Allen[78] extended the work of Ingard to the region of resonance. They took $\chi = -\cot(\omega h/c)$ and used the relationship (148) to relate the rms face velocity to the rms sound pressure. Using a finite difference-approximation to Eq. (23)—with $M = 0$—at two points in the cross section of the duct, they obtained

$$D = -8.7\, Im(k)\, dB = 8.7k\, Im\left\{1 - \frac{4}{k^2}\left[1 + \frac{1}{1-4iz/k} \mp \left(1 + \frac{1}{(1-4iz/k)^2}\right)^{1/2}\right]\right\}^{1/2} dB \qquad (149)$$

for the attenuation over a duct length equal to one half the width of the duct. Although Eq. (149) was derived for an impedance independent of the sound pressure level, they assumed it to hold in the nonlinear case. They found that their analytical solution is in agreement with their experimental results.

2) *Higher modes*

Isakovich[149] determined a second-order expansion for the nonlinear motion of an irrotational, inviscid, compressible gas in a duct lined with a material having linear acoustic properties. He found that the expansion is free of secular terms as opposed to the case of propagation in an unbounded space.

Nayfeh and Tsai[150,151] used the method of multiple scales to determine the nonlinear effects of both the gas and the lining material on the wave propagation in two-dimensional and circular ducts. They used the semi-empirical relationship Eq. (57) to relate the pressure drop to the disturbance velocity across the liner. The potential function was assumed to possess an expansion of the form

$$\Phi = \sum_{n=1}^{3} \varepsilon^n \Phi_n(x_o, x_2, y, t) + 0(\varepsilon^4) \qquad (150)$$

for the two-dimensional duct case and

$$\Phi = \sum_{n=1}^{3} \varepsilon^n \Phi_n(x_o, x_2, r, \theta, t) + 0(\varepsilon^4) \qquad (151)$$

for the circular duct case, where $x_o = x$ and $x_2 = \varepsilon^2 x$, with ε characterizing the amplitude of the wave. Substituting either Eq. (150) or Eq. (151) into Eqs. (126–128) and Eq. (57), eliminating p, ρ and c, and equating coefficients of like powers of ε, they obtained the equations and boundary conditions necessary to solve for each Φ_n. The solution of the first-order problem was written as

$$\Phi_1 = A(x_2)\cos\kappa y \exp[i(kx_o - \omega t)] \qquad (152)$$

for the two-dimensional case and

$$\Phi_1 = A(x_2) J_m(\kappa r) \exp[i(kx_o + m\theta - \omega t)] \qquad (153)$$

for the circular case, where

$$k^2 = \omega^2 - \kappa^2 \qquad (154)$$

and κ is an eigenvalue. The second-order problem was then solved to determine Φ_2. Then an equation was derived for $A(x_2)$ by invoking the solvability condition in the third-order problem. Finally, they obtained an equation for the amplitude of the disturbance of the form

$$da/dx = (-\alpha_o + \varepsilon^2 \alpha_2 a^2)a \qquad (155)$$

where α_o is the linear attenuation rate. Their numerical results show that there exists frequency band widths around the resonant frequencies in which the nonlinearity decreases the attenuation rate and outside which the nonlinearity increases the attenuation rate, in qualitative agreement with experimental observations. Moreover, the effect of the gas nonlinearity increases with increasing sound frequency, whereas the effect of the material nonlinearity decreases with increasing sound frequency.

Instead of representing the effect of the liner by an empirical or semi-empirical impedance, Nayfeh and Tsai[152,153] coupled the wave propagation in the duct with the wave propagation in the liner. They used the method of multiple scales to find an approximate solution to Eqs. (126–129) in the duct and the honeycomb cells and Eqs. (37), (38) and (41) in the porous layer subject to the boundary conditions, (63) and (64), at the duct/liner interface and the honeycomb porous layer interface. The solution of the first-order problem was taken to consist of one mode. Substituting this solution into the second-order problem and using the solvability condition, they obtained an equation describing the amplitude. The result is

$$da/dx = -\alpha_o a + \alpha_1 a^2$$

where a is the amplitude. Numerical evaluation of this result shows good agreement with the experimental result of Kurze and Allen.[78] Moreover, the results show that the nonlinearity flattens and broadens the absorption vs frequency curve, irrespective of the geometrical dimensions or the porous acoustic properties.

References

[1] Greatrex, F. B. and Bridge, R., "The Evolution of the Engine Noise Problem," *Aircraft Engineering*, Vol. 39, Feb. 1967, pp. 6–10.

[2] Ribner, H. S., "Jets and Noise" in *Aerodynamic Noise*, Proceedings of AFOSR-UTIAS Symposium, University of Toronto Press, Toronto, May 1968, pp. 3–42.

[3] Hubbard, H. H., Lansing, D. L., and Runyan, H. L., "A Review of Rotating Blade Noise Technology," *Journal of Sound and Vibration*, Vol. 19, No. 3, Dec. 1971, pp. 227–249.

[4] Osborne, C., "Compressible Unsteady Interactions between Blade Rows," *AIAA Journal*, Vol. 11, No. 3, March 1973, pp. 340–346.

[5] Morfey, C. L., "Rotating Blades and Aerodynamic Noise," *Journal of Sound and Vibration*, Vol. 28, No. 3, June 1973, pp. 587–617.

[6] Schwartz, I. R., "Effects of Rotating Flows on Combustion and Jet Noise," AIAA Paper 72–645, Boston, Mass., June 1972.

[7] Abdelhamid, A. N., Harrje, D. T., Plett, E. G., and Summerfield, M., "Noise Characteristics of Combustion Augmented High-Speed Jets," AIAA Paper 73–189, Washington, D.C., 1973.

[8] Zorumski, W., "Acoustic Theory of Axisymmetric Multisectioned Ducts," TR R-419, 1974, NASA.

[9] Schlichting, H., *Boundary-Layer Theory*, 6th ed., McGraw-Hill, New York, 1968, pp. 61, 254.

[10] Shankar, P. N., "On Acoustic Refraction by Duct Shear Layers," *Journal of Fluid Mechanics*, Vol. 47, Pt. I, May 1971, pp. 81–91.

[11] Möhring, W., "On the Resolution into Modes of Sound Field in Ducts, with Shear Flow," *presented at the Symposium of Acoustics of Flow in Ducts*, University of Southampton, Southampton, England, Jan. 10–14, 1972.

[12] Tester, B. J., "The Optimization of Modal Sound Attenuation in Ducts, in the Absence of Mean Flow," *Journal of Sound and Vibration*, Vol. 27, No. 4, April 1973, pp. 477–513.

[13] Tester, B. J., "The Propagation and Attenuation of Sound in Lined Ducts Containing Uniform or 'Plug' Flow," *Journal of Sound and Vibration*, Vol. 28, No. 2, May 1973, pp. 151–203.

[14] Nayfeh, A. H. and Telionis, D. P., "Algebraically Growing Waves in Ducts with Sheared Mean Flow," *The Journal of the Acoustical Society of America*, Vol. 55, No. 1, Jan. 1974, pp. 16–18.

[15] Zorumski, W. E. and Mason, J. P., "Multiple Eigenvalues of Sound Absorbing Circular and Annular Ducts," *The Journal of the Acoustical Society of America*, Vol. 55, No. 6, June 1974, pp. 1158–1165.

[16] Pridmore-Brown, D. C., "Sound Propagation in a Fluid Flowing Through an Attenuating Duct," *Journal of Fluid Mechanics*, Vol. 4, Aug. 1958, pp. 393–406.

[17] Nayfeh, A. H., *Perturbation Methods*, Wiley-Interscience, New York, 1973.

[18] Mangiarotty, R. A., "Acoustic-Lining Concepts and Materials for Engine Ducts," *The Journal of the Acoustical Society of America*, Vol. 48, No. 3, Sept. 1970, pp. 783–794.

[19] Mangiarotty, R. A., "The Reduction of Aircraft Engine Fan-Compressor Noise Using Acoustic Linings," *Journal of Sound and Vibration*, Vol. 18, No. 4, Oct. 1971, pp. 565–576.

[20] Morse, P. M., *Vibration and Sound*, 2nd ed., McGraw-Hill, New York, 1948, p. 325.

[21] Watson, H. A., "Structural and Environmental Studies of Acoustical Duct-Lining Materials," *The Journal of the Acoustical Society of America*, Vol. 48, No. 3, Pt. 3, Sept. 1970, pp. 795–814.

[22] Lowry, J. G., "The NASA Acoustically Treated Nacelle Program," *The Journal of the Acoustical Society of America*, Vol. 48, No. 3, Pt. 3, Sept. 1970, pp. 780–782.

[23] Marsh, A. H., "Application of Duct-Lining Technology to Jet Aircraft," *The Journal of the Acoustical Society of America*, Vol. 48, No. 3, Pt. 3, Sept. 1970, pp. 826–842.

[24] Atvars, J. and Mangiarotty, R. A., "Parametric Studies of the Acoustic Behavior of Duct-Lining Materials," *The Journal of the Acoustical Society of America*, Vol. 48, No. 3, Pt. 3, Sept. 1970, pp. 815–825.

[25] Irmay, S., "On the Theoretical Derivation of Darcy and Forchheimer Formula," *American Geophysical Union, Transactions*, Vol. 39, No. 4, Aug. 1958, pp. 702–707.

[26] Scott, R. A., "The Absorption of Sound in a Homogeneous Porous Medium," *Proceedings of the Physical Society*, London, Vol. 58, March 1946, pp. 165–183.

[27] Morse, P. M. and Ingard, K. U., *Theoretical Acoustics*, McGraw-Hill, New York, 1968.

[28] Zwikker, C. and Kosten, C. W., *Sound Absorbing Materials*, Elsevier, New York, 1949.

[29] Scheidegger, A. E., *The Physics of Flow Through Porous Media*, Macmillan, New York, 1957.

[30] Beranek, L. L., "Acoustical Properties of Homogeneous, Isotropic Tiles and Flexible Blankets," *The Journal of the Acoustical Society of America*, Vol. 19, No. 4, July 1947, pp. 556–568.

[31] Tack, D. H. and Lambert, R. F., "Influence of Shear Flow on Sound Attenuation in a Lined Duct," *The Journal of the Acoustical Society of America*, Vol. 38, No. 4, Oct. 1965, pp. 655–666.

[32] Bies, D. A., "Acoustical Properties of Porous Materials," *Noise and Vibration Control*, edited by L. L. Beranek, McGraw-Hill, New York, 1971, pp. 245–269.

[33] Green, L. and Duwez, P., "Fluid Flow Through Porous Metals," *Journal of Applied Mechanics*, Vol. 18, No. 1, March 1951, pp. 39–45.

[34] Mongy, M., "Acoustical Properties of Porous Materials," *Acustica*, Vol. 28, No. 4, April 1973, pp. 243–247.

[35] Bokor, A., "A Comparison of Some Acoustic Duct Lining Materials, According to Scott's Theory," *Journal of Sound and Vibration*, Vol. 14, No. 3, Feb. 1971, pp. 367–373.

[36] Kurze, U. J. and Vér, I. L., "Sound Attenuation in Ducts Lined with Non-isotropic Material," *Journal of Sound and Vibration*, Vol. 24, No. 2, Sept. 1972, pp. 177–187.

[37] Kaiser, J. E., Shaker, B., and Nayfeh, A. H., "Influence of Liner Thickness on Wave Propagation in Ducts," Rept. No. E-74-8, Virginia Polytechnic Institute and State University, Blacksburg, Va.; also *Journal of Sound and Vibration*, 1974, to be published.

[38] Zorumski, W. E., "Acoustic Impedance of Curved Multi-Layered Duct Liners," TN D-7277, 1973, NASA.

[39] Mariano, S., "Effect of Wall Shear Layers on the Sound Attenuation by Broad Band-Width Linings," *Acustica*, Vol. 29, No. 3, Sept. 1973, pp. 148–156.

[40] Ko, S.-H., "Theoretical Prediction of Sound Attenuation in Acoustically Lined Annular Ducts in the Presence of Uniform Flow and Shear Flow," *The Journal of the Acoustical Society of America*, Vol. 54, No. 6, Dec. 1973, pp. 1592–1606.

[41] Nayfeh, A. H., Sun, J., and Telionis, D. P., "Effect of Bulk Liners on Wave Propagation in Ducts," *AIAA Journal*, Vol. 12, No. 6, June 1974, pp. 838–843.

[42] Bokor, A., "Attenuation of Sound in Lined Ducts," *Journal of Sound and Vibration*, Vol. 10, No. 3, Nov. 1969, pp. 390–403.

[43] Leskov, E. A., Osirov, G. L., and Yudin, E. K., "Experimental Investigations of Splitter Duct Silencers," *Applied Acoustics*, Vol. 3, No. 1, Jan. 1970, pp. 47–56.

[44] Walsdorff, J., "Absorptionsschalldämpfer ohne Kassettierung," Paper 25A6, 1971, *Seventh International Congress on Acoustics*, Vol. II, Budapest, Hungary, 1971, pp. 257–260.

[45] Melling, T. H., "The Acoustic Impedance of Perforates at Medium and High Sound Pressure Levels," *Journal of Sound and Vibration*, Vol. 29, No. 1, July 1973, pp. 1–65.

[46] Rice, E. J., "A Model for the Pressure Excitation Spectrum and Acoustic Impedance of Sound Absorbers in the Presence of Grazing Flow," AIAA Paper 73-995, Seattle, Wash., 1973.

[47] Zorumski, W. E. and Parrott, T. L., "Non-Linear Acoustic Theory for Rigid Porous Materials," TN-6196, 1971, NASA.

[48] Miles, J. W., "On the Reflection of Sound at an Interface of Relative Motion," *The Journal of the Acoustical Society of America*, Vol. 29, No. 2, Feb. 1957, pp. 226–228.

[49] Ribner, H. S., "Reflection, Transmission, and Amplification of Sound by a Moving Medium," *The Journal of the Acoustical Society of America*, Vol. 29, No. 4, April 1957, pp. 435–441.

[50] Ingard, U., "Influence of Fluid Motion Past a Plane Boundary on Sound Reflection, Absorption and Transmission," *The Journal of the Acoustical Society of America*, Vol. 31, No. 7, July 1959, pp. 1035–1036.

[51] Gottlieb, P., "Sound Transmission Through a Velocity Discontinuity," *The Journal of the Acoustical Society of America*, Vol. 31, No. 7, July 1959, pp. 1036–1037.

[52] Mechel, F. and Mertens, P., "Schallausbreitung in Absorbierend Ausgekleideten Strömungskanälen bei Hohen Windgeschwindigkeiten," *Acustica*, Vol. 13, 1963, pp. 154–165.

[53] Mungur, P. and Plumblee, H. E., *Propagation and Attenuation of Sound in a Soft-walled Annular Duct Containing a Sheared Flow*, SP-207, 1969, pp. 305–327, NASA.

[54] Savkar, S. D., "Propagation of Sound in Ducts with Shear Flow," *Journal of Sound and Vibration*, Vol. 19, No. 3, Dec. 1971, pp. 355–372.

[55] Eversman, W. and Beckemeyer, R. J., "Transmission of Sound in Ducts with Thin Shear Layers-Convergence to the Uniform Flow Case," *The Journal of the Acoustical Society of America*, Vol. 52, No. 1, Pt. 2, July 1972, pp. 216–220.

[56] Tester, B. J., "Some Aspects of 'Sound' Attenuation in Lined Ducts Containing Inviscid Mean Flows with Boundary Layers," *Journal of Sound and Vibration*, Vol. 28, No. 2, May 1973, pp. 217–245.

[57] Nayfeh, A. H., Kaiser, J. E., and Shaker, B. S., "Effect of Mean-Velocity Profile Shapes on Sound Transmission Through Rectangular Ducts," *Journal of Sound and Vibration*, Vol. 34, No. 3, June 1974, pp. 413–423.

[58] Rice, E. J., *Propagation of Waves in an Acoustically Lined Duct with a Mean Flow*, SP-207, 1969, pp. 345–355, NASA.

[59] Doak, P. E. and Vaidya, P. G., "Attenuation of Plane Wave and Higher Order Mode Sound Propagation in Lined Ducts," *Journal of Sound and Vibration*, Vol. 12, No. 2, June 1970, pp. 201–224.

[60] Eversman, W., "The Effect of Mach Number on the Tuning of an Acoustic Lining in a Flow Duct," *The Journal of the Acoustical Society of America*, Vol. 48, No. 2, Part 1, Aug. 1970, pp. 425–427.

[61] Ko, S.-H., "Sound Attenuation in Lined Rectangular Ducts with Flow and Its Application to the Reduction of Aircraft Engine Noise," *The Journal of the Acoustical Society of America*, Vol. 50, No. 6, Pt. 1, Dec. 1971, pp. 1418–1432.

[62] Tyler, J. M. and Sofrin, T. G., "Axial Flow Compressor Noise Studies," *SAE Transactions*, Vol. 70, 1962, pp. 309–332.

[63] Kester, J. D. and Slaiby, T. G., "Designing the JT9D Engine

to Meet Low Noise Requirements for Future Transports," SAE Paper 670331, April 1967.

[64] Morfey, C. L., "Sound Transmission and Generation in Ducts with Flow," *Journal of Sound and Vibration*, Vol. 14, No. 1, Jan. 1971, pp. 37–55.

[65] Abramowitz, M. and Stegun, I. A., eds., *Handbook of Mathematical Functions, with Formulas, Graphs and Mathematical Tables*, Applied Mathematical Series, National Bureau of Standards, 1964.

[66] Eversman, W., "Representation of a $1/N$ Power-Law Boundary Layer in the Sheared Flow Acoustic Transmission Problem," *Journal of Sound and Vibration*, Vol. 24, No. 4, Oct. 1972, pp. 459–469.

[67] Eversman, W., "Approximation for Thin Boundary Layers in the Sheared Flow Duct Transmission Problem," *The Journal of the Acoustical Society of America*, Vol. 53, No. 5, May 1973, pp. 1346–1350.

[68] Beckemeyer, R. J., "On the Effect of Thin Shear Layers with Flow and Density Gradients on Small Disturbances in Inviscid, Compressible Flows," *Journal of Sound and Vibration*, Vol. 31, No. 2, Nov. 1973, pp. 251–256.

[69] Hersh, A. S. and Catton, I., "Effect of Shear Flow on Sound Propagation in Rectangular Ducts," *The Journal of the Acoustical Society of America*, Vol. 50, No. 3, Pt. 2, Sept. 1971, pp. 992–1003.

[70] Rice, E. J., "Attenuation of Sound in Soft-Walled Circular Ducts," in *Aerodynamic Noise*, Proceedings of the AFOSR-UTIAS Symposium, University of Toronto Press, Toronto, 1968, pp. 229–249.

[71] Eversman, W., "Effect of Boundary Layer on the Transmission and Attenuation of Sound in an Acoustically Treated Circular Duct," *The Journal of the Acoustical Society of America*, Vol. 49, No. 5, May 1971, pp. 1372–1380.

[72] Mikhail, M. N. and Abdelhamid, A. N., "A Rapid Method for the Solution of Acoustic Propagation in Ducts Containing Shear Flow," Rept. ME 73–3, Carleton University, Ottawa, Ontario, Aug. 1973.

[73] Mungur, P. and Gladwell, G. M. L., "Acoustic Wave Propagation in a Sheared Fluid Contained in a Duct," *Journal of Sound and Vibration*, Vol. 9, No. 1, Jan. 1969, pp. 28–48.

[74] Shankar, P. N., "Sound Propagation in Duct Shear Layers," *Journal of Sound and Vibration*, Vol. 22, No. 2, May 1972, pp. 221–232.

[75] Shankar, P. N., "Acoustic Refraction and Attenuation in Cylindrical and Annular Ducts," *Journal of Sound and Vibration*, Vol. 22, No. 2, May 1972, pp. 233–246.

[76] Mikhail, M. N. and Abdelhamid, A. N., "Shear Flow Effect on the Propagation and Attenuation of Sound Waves in an Acoustically Treated Annular Duct," Rept. ME-73-2, March 1973, Carleton University, Ottawa, Ontario.

[77] Mikhail, M. N. and Abdelhamid, A. N., "Transmission and Far-Field Radiation of Sound Waves in and from Lined Ducts Containing Shear Flow," AIAA Paper 73-1013, Seattle, Wash., Oct. 1973.

[78] Kurze, U. J. and Allen, C. H., "Influence of Flow and High Sound Level on the Attenuation in a Lined Duct," *The Journal of the Acoustical Society of America*, Vol. 49, No. 5, Pt. 2, May 1971, pp. 1643–1653.

[79] Mariano, S., "Effect of Wall Shear Layers on the Sound Attenuation in Acoustically Lined Rectangular Ducts," *Journal of Sound and Vibration*, Vol. 19, No. 3, Dec. 1971, pp. 261–275.

[80] Ko, S.-H., "Sound Attenuation in Acoustically Lined Circular Ducts in the Presence of Uniform Flow and Shear Flow," *Journal of Sound and Vibration*, Vol. 22, No. 2, May 1972, pp. 193–210.

[81] Mariano, S., "Sound Absorption in Lined Rectangular Ducts with Wall Shear Layers—Convergence of the Numerical Procedure to the Analytical Solution," *Journal of Sound and Vibration*, Vol. 27, March 1973, pp. 123–127.

[82] Kaiser, J. E., "Comparison of Central-Difference and Forward-Integration Techniques for Sound Propagation in Lined Ducts," Rept. E-73-30, 1973, Virginia Polytechnic Institute and State University Blacksburg, Va.

[83] Ames, W. F., *Numerical Methods for Partial Differential Equations*, Barnes & Noble, New York, 1969.

[84] Unruh, J. F. and Eversman, W., "The Utility of the Galerkin Method for the Acoustic Transmission in an Attenuating Duct," *Journal of Sound and Vibration*, Vol. 23, No. 2, July 1972, pp. 187–197.

[85] Unruh, J. F. and Eversman, W., "The Transmission of Sound in an Acoustically Treated Rectangular Duct with Boundary Layer," *Journal of Sound and Vibration*, Vol. 25, No. 3, Dec. 1972, pp. 371–382.

[86] Mariano, S., "Optimization of Acoustic Linings in Presence of Wall Shear Layers," *Journal of Sound and Vibration*, Vol. 23, No. 2, July 1972, pp. 229–235.

[87] Feder, E. and Dean, L. W., "Analytical and Experimental Studies for Predicting Noise Attenuation in Acoustically Treated Ducts for Turbo-Fan Engines," CR-1373, 1969, NASA.

[88] Plumblee, H. E., "A Theoretical and Experimental Study of Sound Attenuation in an Annular Duct," AIAA Paper 73-1005, Seattle, Wash., Oct. 1973.

[89] Dean, P. D., "On the Measurement of the Local Impedance of the Walls of Flow Ducts and Its Use in Predicting Sound Attenuation," Ph.D. thesis, University of Southampton, Southampton, England, 1972.

[90] Plumblee, H. E. and Dean, P. D., "Sound Measurements Within and in the Radiated Field of an Annular Duct with Flow," *Journal of Sound and Vibration*, Vol. 28, No. 4, June 1973, pp. 715–735.

[91] Plumblee, H. E., Dean, P. D., Wynne, G. A., and Burrin, R. H., "Sound Propagation in and Radiation from Acoustically Lined Flow Ducts: A Comparison of Experiment and Theory," CR-2306, 1973, NASA.

[92] Doak, P. E., "Fundamentals of Aerodynamic Sound Theory and Flow Duct Acoustics," *Journal of Sound and Vibration*, Vol. 28, No. 3, June 1973, pp. 527–561.

[93] Kapur, A. and Mungur, P., "Sound Interaction with a Helical Flow Contained in an Annular Duct with Radial Gradients of Flow, Density and Temperature," AIAA Paper 73-1010, Seattle, Wash., 1973.

[94] Lord Rayleigh, *Theory of Sound*, Vol. II, Dover, New York, 1945, pp. 66–68.

[95] Cremer, L., "Über die Akustische Grenzschicht vor Starren Wänden," *Archiv der Elektrischen Übertragung*, Vol. 2, 1948, pp. 136–139.

[96] Beatty, R. E. J., "Boundary Layer Attenuation of Higher-Order Modes in Rectangular and Circular Tubes," *The Journal of the Acoustical Society of America*, Vol. 22, Nov. 1950, pp. 850–854.

[97] Shaw, E. A. G., "The Attenuation of the Higher Modes of Acoustic Waves in a Rectangular Tube," *Acustica*, Vol. 3, 1953, pp. 87–95.

[98] Lambert, R. F., "A Study of the Factors Influencing the Damping of an Acoustical Cavity Resonator," *The Journal of the Acoustical Society of America*, Vol. 25, No. 6, Nov. 1953, pp. 1068–1083.

[99] Nayfeh, A. H., "Effect of the Acoustic Boundary Layer on the Wave Propagation in Ducts," *The Journal of the Acoustical Society of America*, Vol. 54, No. 6, Dec. 1973, pp. 1737–1742.

[100] Pestorius, F. M. and Blackstock, D. T., "Non-Linear Distortion in the Propagation of Intense Acoustic Noise," *Interagency Symposium on University Research in Transportation Noise Proceedings*, Vol. II, March 1973, Stanford University, Stanford, Calif., pp. 565–577.

[101] Mungur, P., and Tree, D., "Sound Propagation in Sheared Flow in a Duct with Transverse Temperature Gradients," Paper 24 P7, *Seventh International Congress on Acoustics*, Vol. IV, Budapest, Hungary, 1971, pp. 349–353.

[102] Kapur, A. and Mungur, P., "On the Propagation of Sound in a Rectangular Duct with Gradients of Mean Flow and Temperature in Both Transverse Directions," *Journal of Sound and Vibration*, Vol. 23, No. 3, Aug. 1972, pp. 401–404.

[103] Kapur, A., Cummings, A., and Mungur, P., "Sound Propagation in a Combustion Can with Axial Temperature and Density Gradients," *Journal of Sound and Vibration*, Vol. 25, No. 1, Nov. 1972, pp. 129–138.

[104] Nayfeh, A. H. and Sun, J., "Effect of Transverse Velocity and Temperature Gradients on Sound Attenuation in Rectangular Ducts," *Journal of Sound and Vibration*, Vol. 34, No. 4, June 1974, pp. 505–517.

[105] Webster, A. G., "Acoustical Impedance and the Theory of Horns and of the Phonograph," *Proceedings of the National Academy of Science*, Vol. 5, July 1919, pp. 275–282.

[106] Kinsler, L. E. and Frey, A. R., *Fundamentals of Acoustics*, 2nd ed., Wiley, New York, 1962.

[107] Peube, J. L. and Chasseriaux, J., "Nonlinear Acoustics in Ducts with Varying Cross Section," *Journal of Sound and Vibration*, Vol. 27, No. 4, April 1973, pp. 533–548.

[108] Beckemeyer, R. J. and Eversman, W., "Computational Method for Studying Acoustic Propagation in Nonuniform Waveguides" AIAA Paper 73-1006, Seattle, Wash., 1973.

[109] Stevenson, A. F., "Exact and Approximate Equations for Wave Propagation in Acoustic Horns," *Journal of Applied Physics*, Vol. 22, No. 12, Dec. 1951, pp. 1461–1463.

[110] Miles, J., "The Reflection of Sound due to a Change in Cross-Section of a Circular Tube," *The Journal of the Acoustical Society of America*, Vol. 26, No. 3, March 1954, pp. 14–19.

[111] Zorumski, W. E. and Clark, L. R., "Sound Radiation from a Source in an Acoustically Treated Circular Duct," unpublished, 1971, NASA Langley Research Center, Hampton, Va.

[112] Lansing, D. L. and Zorumski, W. E., "Effects of Wall Admittance Changes on Duct Transmission and Radiation of Sound," *Journal of Sound and Vibration*, Vol. 27, No. 1, March 1973, pp. 85–100.

[113] Alfredson, R. J., "The Propagation of Sound in a Circular

Duct of Continuously Varying Cross-Sectional Area," *Journal of Sound and Vibration*, Vol. 23, No. 4, Aug. 1972, pp. 433–442.

[114] Nayfeh, A. H. and Telionis, D. P., "Acoustic Propagation in Ducts with Varying Cross-Sections," *The Journal of the Acoustical Society of America*, Vol. 54, No. 6, Dec. 1973, pp. 1654–1661.

[115] Isakovitch, M. A., "Scattering of Sound Waves on Small Irregularities in a Wave Guide," *Akusticheskii Zhurnal*, Vol. 3, 1957, pp. 37–45.

[116] Samuels, J. S. "On Propagation of Waves in Slightly Rough Ducts," *The Journal of the Acoustical Society of America*, Vol. 31, March 1959, pp. 319–325.

[117] Salant, R. F., "Acoustic Propagation in Waveguides with Sinusoidal Walls," *The Journal of the Acoustical Society of America*, Vol. 53, Feb. 1973, pp. 504–507.

[118] Nayfeh, A. H., "Sound Waves in Two-Dimensional Ducts with Sinusoidal Walls," *The Journal of the Acoustical Society of America*, Vol. 56, No. 3, Sept. 1974, pp. 768–770.

[119] Large, J. B., Wilby, J. F., Grande, E., and Anderson, A. O., "The Development of Engineering Practices in Jet, Compressor and Boundary Layer Noise," *Aerodynamic Noise*, Proceedings of the AFOSR-UTIAS Symposium on Aerodynamic Noise, Toronto University Press, Toronto, May 1968, pp. 43–67.

[120] Chestnut, D. and Clark, L. R., "Noise Reduction by Means of Variable-Geometry Inlet Guide Vanes in a Cascade Apparatus," TM X-2392, 1971, NASA.

[121] King, L. S. and Karamcheti, K., "Propagation of Plane Waves in the Flow Through a Variable Area Duct," AIAA Paper 73-1009, Seattle, Wash., 1973.

[122] Baumeister, K. J. and Rice, E. J., "A Difference Theory for Noise Propagation in an Acoustically Lined Duct with Mean Flow," AIAA Paper 73-1007, Seattle, Wash., 1973.

[123] Whitham, G. B., "On the Propagation of Shock Waves Through Regions of Non-Uniform Area or Flow," *Journal of Fluid Mechanics*, Vol. 4, Pt. 4, Aug. 1958, pp. 337–360.

[124] Rudinger, G., "Passage of Shock Waves Through Ducts of Variable Cross Section," *Physics of Fluids*, Vol. 3, No. 3, May–June, 1960, pp. 449–455.

[125] Powell, A., "Propagation of a Pressure Pulse in a Compressible Flow," *The Journal of the Acoustical Society of America*, Vol. 31, No. 11, Nov. 1959, pp. 1527–1535.

[126] Powell, A. "Theory of Sound Propagation through Ducts Carrying High-Speed Flows," *The Journal of the Acoustical Society of America*, Vol. 32, No. 12, Dec. 1960, pp. 1640–1646.

[127] Eisenberg, N. A. and Kao, T. W., "Propagation of Sound Through a Variable-Area Duct with a Steady Compressible Flow," *The Journal of the Acoustical Society of America*, Vol. 49, No. 1, Jan. 1971, pp. 169–175.

[128] Davis, S. S. and Johnson, M. L., "Propagation of Plane Waves in a Variable Area Duct Carrying a Compressible Subsonic Flow," presented at the 87th Meeting of the Acoustical Society of America, New York, 1974.

[129] Kooker, D. E., and Zinn, B. T., "Use of a Relaxation Technique in Nozzle Wave Propagation Problems," AIAA Paper 73-1011, Seattle, Wash., 1973.

[130] Hogge, H. D. and Ritzi, E. W., "Theoretical Studies of Sound Emission from Aircraft Ducts," AIAA Paper 73-1012, Seattle, Wash., 1973.

[131] Huerre, P. and Karamcheti, K., "Propagation of Sound through a Fluid Moving in a Duct of Varying Area," *Interagency Symposium of University Research in Transportation Noise Proceedings*, Vol. II, March 1973, Stanford University, Stanford, Calif., pp. 397–413.

[132] Tam, C. K. W., "Transmission of Spinning Acoustic Modes in a Slightly Nonuniform Duct," *Journal of Sound and Vibration*, Vol. 18, No. 3, Oct. 1971, pp. 339–351.

[133] Nayfeh, A. H., Telionis, D. P., and Lekoudis, S. G., "Acoustic Propagation in Ducts with Varying Cross Sections and Sheared Mean Flow," AIAA Paper 73-1008, Seattle, Wash., 1973.

[134] Nayfeh, A. H., Kaiser, J. E., and Telionis, D. P., "Transmission of Sound Through Annular Ducts of Varying Cross Sections and Sheared Mean Flow," AIAA Paper 74-58, Washington, D.C., Jan. 1974; also, *AIAA Journal*, Vol. 13, No. 1, Jan. 1975, pp. 60–65.

[135] Tsien, H. S., "The Equations of Gas Dynamics," in *Fundamentals of Gasdynamics*, edited by Emmons, H. W., Princeton University Press, Princeton, New Jersey, 1958, pp. 36–37.

[136] Fay, R. D., "Plane Sound Waves of Finite Amplitude," *The Journal of the Acoustical Society of America*, Vol. 3, Oct. 1931, pp. 222–241.

[137] Fubini, G. E., "Anomalie Nella Propagazione di onde Acustische die Grande Ampiezza," *Alta Frequenza*, Vol. 4, 1935, pp. 530–581.

[138] Blackstock, D. T., "Connection between the Fay and Fubini Solutions for Plane Sound Waves of Finite Amplitude," *The Journal of the Acoustical Society of America*, Vol. 39, No. 6, June 1966, pp. 1019–1026.

[139] Coppens, A. B., "Theoretical Study of Finite-Amplitude Traveling Waves in Rigid-Walled Ducts: Behavior for Strengths Precluding Shock Formation," *The Journal of the Acoustical Society of America*, Vol. 49, No. 1, Part 2, Jan. 1971, pp. 306–318.

[140] Maslen, S. H. and Moore, F. K., "On Strong Transverse Waves Without Shocks in a Circular Cylinder," *Journal of Aeronautical Sciences*, Vol. 23, June 1956, pp. 583–593.

[141] Burns, S. H., "Finite-Amplitude Distortion in Air at High Acoustic Pressures," *The Journal of the Acoustical Society of America*, Vol. 41, No. 4, April 1967, pp. 1157–1169.

[142] Keller, J. B. and Millman, M. H., "Finite-Amplitude Sound-Wave Propagation in a Waveguide," *The Journal of the Acoustical Society of America*, Vol. 49, No. 1, Pt. 2, Jan. 1971, pp. 329–333.

[143] Keller, J. B., "Nonlinear Forced and Free Vibrations in Acoustic Waveguides," *The Journal of the Acoustical Society of America*, Vol. 55, March 1974, pp. 524–527.

[144] Nayfeh, A. H., "Nonlinear Propagation of a Wave-Packet in a Hard-Walled Circular Duct," Rept. E-74-9, Virginia Polytechnic Institute and State University, Blacksburg, Va., 1974.

[145] Zorumski, W. E. and Parrott, T. L., *Nonlinear Acoustic Theory for Thin Porous Sheets*, SP-189, 1968, pp. 17–27, NASA.

[146] Ingard, U., "Nonlinear Attenuation of Sound in a Duct," *The Journal of the Acoustical Society of America*, Vol. 43, No. 1, Jan. 1968, pp. 167–168.

[147] Ingard, U., "Absorption Characteristics of Nonlinear Acoustic Resonators," *The Journal of the Acoustical Society of America*, Vol. 44, No. 4, Oct. 1968, pp. 1155–1156.

[148] Ingard, U. and Ising, H., "Acoustic Nonlinearity of an Orifice," *The Journal of the Acoustical Society of America*, Vol. 42, No. 1, July 1967, pp. 6–17.

[149] Isakovich, M. S., "Nonlinear Effects Involved in Certain Acoustical Problems," *Soviet Physics-Acoustics*, Vol. 6, No. 3, 1960, pp. 321–325.

[150] Nayfeh, A. H. and Tsai, M.-S., "Nonlinear Acoustic Propagation in Two-Dimensional Ducts," *The Journal of the Acoustical Society of America*. Vol. 55, June 1974, pp. 1166–1172.

[151] Nayfeh, A. H. and Tsai, M.-S., "Nonlinear Wave Propagation in Acoustically Lined Circular Ducts," *Journal of Sound and Vibration*, Vol. 36, Nov. 1974, pp. 77–89.

[152] Nayfeh, A. H. and Tsai, M.-S., "Finite-Amplitude Waves in Two-Dimensional Lined Ducts," *Journal of Sound and Vibration*, Vol. 36, Nov. 1974, pp. 27–38.

[153] Nayfeh, A. H. and Tsai, M.-S., "Finite Amplitude Waves in Cylindrical Lined Ducts," AIAA Paper 74-553, Palo Alto, Calif., 1974